arXiv:nucl-th/9509002v1 1 Sep 1995

Nuclear muon capture by ^{3}He: meson exchange currents for the triton channel

J.G.Congleton*
Department of Physics, University of Newcastle, Newcastle upon Tyne, NE1 7RU, UK.

E.Truhlík†
Inst. of Nuclear Physics, Academy of Sciences of the Czech Republic,
CZ 250 68 Řež near Prague, Czech Republic.

(February 9, 2008)

Abstract

We have calculated exchange corrections for nuclear muon capture by ^{3}He leading to the ^{3}H final state using the hard-pion model and realistic nuclear wavefunctions. These currents modify the vector and axial part of the weak nuclear current. In their absence the rate is 12% smaller than found by experiment.

Our final result for the rate is 1502 ± 32 per second. For the analyzing powers we find $A_v = 0.515 \pm 0.005$, $A_t = -0.375 \pm 0.004$ and $A_\Delta = -0.110 \pm 0.006$. These predictions use the PCAC value of g_P. The variation of the observables with g_P is also reported.

PACS numbers: 23.40

Typeset using REVTEX

---

[*] Supported by the Sir James Knott Fellowship.

[†] Supported by grants Nos. 202/94/0370 (GA CR) and 148410 (GA ASC CR).

I. INTRODUCTION

As has recently been discussed in Ref. [1], the reaction of negative muon capture by the helion,

$$\mu^- + {}^3\mathrm{He} \to \nu_\mu + {}^3\mathrm{H} \tag{1.1}$$

is at present potentially able to provide us with the induced pseudoscalar coupling g_P with nearly the same precision as from capture by a free proton. Indeed, accurate three-nucleon wavefunctions are now available and the uncertainties due to the description of the nuclear states can be reduced to a minimum.

However, the calculations reported in Refs. [2,3] for other weak reactions on light nuclei show that besides the one–nucleon contribution, meson exchange current (MEC) effects should be taken into account. That this is so can also be seen from the analysis performed in Ref. [1], where Congleton and Fearing compared the results obtained using the elementary particle model (EPM) to the standard calculations in the impulse approximation (IA): the effective magnetic couplings G_P and G_A are 10% smaller in the IA (see Table I). Table II shows the contributions of the current components to the effective couplings, and it can be seen that $\vec{j}_A$ makes an important contribution to G_P and G_A.

Here we continue the study of the characteristics of reaction (1.1) and consider the weak MEC effects. For the operator of the weak axial nuclear MEC we adopt the one published recently in Ref. [4], which was applied earlier to negative muon capture by deuterons in Ref. [2]. The weak axial nuclear MEC operator satisfies the nuclear continuity equation (PCAC) up to the order considered, which is $1/M^2$ (M is the nucleon mass). The space-like component of the operator contains both static and velocity dependent parts. We take into account fully both the static part and the terms linear in external momenta from the velocity dependent part.

Further, we use for the vector part of the weak MEC operator the standard isovector currents well known from the electromagnetic processes [5–9]. We employ non–relativistic operators satisfying CVC at order $1/M$.

A brief account of the work has been recently reported in Ref. [10]. Here we present the full results. In section II, we discuss the formalism employed, section III contains the numerical analysis of the studied problem and in section IV we give our conclusions. The most important of them is that including the weak axial and vector π-MEC in the microscopic calculation yields results which agree closely with the EPM in their predictions for observables.

In order to make the paper more transparent, we postpone necessary details of the formalism and partial results into a series of appendices.

II. FORMALISM

To evaluate the effect of meson exchange currents, the ${}^3\mathrm{H} \to {}^3\mathrm{He}$ weak nuclear current was parameterized by six Q dependent current amplitudes $\rho_0, \rho_1, j_Q, j_\sigma, j_\times^{(1)}$ and $j_\times^{(2)}$ as follows.

$$\langle\, {}^3\mathrm{H}; m_f \mid j^0 \mid {}^3\mathrm{He}; m_i \,\rangle = \chi^\dagger_{m_f}\Big\{\rho_0 + \rho_1 \hat{Q}\cdot\vec{\sigma}\Big\}\chi_{m_i} \tag{2.1a}$$

$$\langle\, {}^3\mathrm{H}; m_f \mid \vec{j} \mid {}^3\mathrm{He}; m_i \,\rangle = \chi^\dagger_{m_f}\Big\{j_Q\hat{Q} + j^{(1)}_\times i\hat{Q}\times\vec{\sigma} + j_\sigma\vec{\sigma} + j^{(2)}_\times[\hat{Q}(\hat{Q}\cdot\vec{\sigma}) - \tfrac{1}{3}\vec{\sigma}]\Big\}\chi_{m_i} \tag{2.1b}$$

In Eqs. (2.1), m_i and m_f are the initial and final projections of the internal nuclear angular momentum, j^0 and $\vec{j}$ are the time and space components of the total weak four current and the three-momentum transfer to the helion is $\vec{Q}$. The current amplitudes are not relativistically invariant and are not independent (if we make the assumption that second class currents are absent). To see the non-independence note that the EPM parameterizes the current using only four form factors whereas there are six current amplitudes. The current amplitudes are, however, useful in the formulation because there exists a simple correspondence between the non-relativistic current operators and the current amplitude to which the matrix element of that operator contributes.

The total current has a vector and an axial part. The vector part contributes to $\rho_0, j_Q, j^{(1)}_\times$ and the axial part to $\rho_1, j_\sigma, j^{(2)}_\times$. The relationships between these current amplitudes and the traditional effective form factors G_V, G_P and G_A are,

$$G_V = \rho_0 + j_Q \tag{2.2a}$$

$$G_P = j^{(1)}_\times - j^{(2)}_\times - \rho_1 \tag{2.2b}$$

$$G_A = j^{(1)}_\times + j_\sigma - \frac{1}{3}j^{(2)}_\times . \tag{2.2c}$$

The statistical capture rate Γ_0 and analyzing powers A_v, A_t and A_Δ for reaction (1.1) can be found from the effective form factors by using Eqs. (3)(11)(12) and (13) of Ref. [1].

Our model for the nuclear current employs non-relativistic wavefunctions and current operators the latter of which are listed in appendix A. After suffering a multipole decomposition of the plane wave factor, the current operators yielded matrix elements with the following five forms,

$$Z^J_{l\lambda L} = \langle\, {}^3\mathrm{H} \mid\mid [4\pi\mathcal{Y}^L_{l\lambda}(\hat{x}\hat{y})\otimes S_\Sigma]_J\, j_\lambda(Qy/3)\mathcal{I} \mid\mid {}^3\mathrm{He}\,\rangle/(2J+1)^{1/2} \tag{2.3a}$$

$${}_xZ^J_{l\lambda L} = \langle\, {}^3\mathrm{H} \mid\mid [4\pi\mathcal{Y}^L_{l\lambda}(\hat{x}\hat{y})\otimes S_\Sigma]_J\, j_\lambda(Qy/3)\mathcal{I}\frac{\partial}{\partial x_\pi} \mid\mid {}^3\mathrm{He}\,\rangle/(2J+1)^{1/2} \tag{2.3b}$$

$${}_yZ^J_{l\lambda L} = \langle\, {}^3\mathrm{H} \mid\mid [4\pi\mathcal{Y}^L_{l\lambda}(\hat{x}\hat{y})\otimes S_\Sigma]_J\, j_\lambda(Qy/3)\mathcal{I}\frac{\partial}{\partial y_\pi} \mid\mid {}^3\mathrm{He}\,\rangle/(2J+1)^{1/2} \tag{2.3c}$$

$${}_xZ^{K1J}_{l\lambda L} = \langle\, {}^3\mathrm{H} \mid\mid \Big[[4\pi\mathcal{Y}^L_{l\lambda}(\hat{x}\hat{y})\otimes S_\Sigma]_K \otimes \frac{\hat{\nabla}_x}{x_\pi}\Big]_J\, j_\lambda(Qy/3)\mathcal{I} \mid\mid {}^3\mathrm{He}\,\rangle/(2J+1)^{1/2} \tag{2.3d}$$

$${}_yZ^{K1J}_{l\lambda L} = \langle\, {}^3\mathrm{H} \mid\mid \Big[[4\pi\mathcal{Y}^L_{l\lambda}(\hat{x}\hat{y})\otimes S_\Sigma]_K \otimes \frac{\hat{\nabla}_y}{y_\pi}\Big]_J\, j_\lambda(Qy/3)\mathcal{I} \mid\mid {}^3\mathrm{He}\,\rangle/(2J+1)^{1/2}. \tag{2.3e}$$

The letter Z takes on values $A \dots I$ according to the spin and isospin operators S_Σ and $\mathcal{I}$ as indicated in Table III. For example, the Gamow-Teller matrix element is $1/4\ F^1_{000}$. The matrix elements are reduced in the spin-spatial part but not in the isospin part so that for example,

$$\langle\, {}^3\mathrm{He}\, ||\, 3\tau^z_3\, ||\, {}^3\mathrm{He}\,\rangle = +1 \tag{2.4a}$$

$$\langle\, {}^3\mathrm{H}\, ||\, 3\tau^z_3\, ||\, {}^3\mathrm{H}\,\rangle = -1. \tag{2.4b}$$

The following selection rules were applied to the matrix elements.

1. Parity. For $Z^J_{l\lambda L}$ this implies that only matrix elements with, $l + \lambda =$ even, are significant.

2. Hermiticity and isospin symmetry. Because ^{3}He and ^{3}H form a good isospin doublet, matrix elements $Z^J_{l\lambda L}$ with an anti-hermitian operator are insignificant. This approximation is good at the few $\times 10^{-3}$ level since we have for the wavefunctions used here, (which have no isospin 3/2 components),

   $$\langle\, {}^3\mathrm{H}\, ||\, 3I^-_3\, ||\, {}^3\mathrm{He}\,\rangle = 0.9998 \tag{2.5}$$

   and further the probability of the $I = 3/2$ components is $10^{-5} - 10^{-6}$ [11]. For the local matrix elements A, C, D, E, F this implies that only $J = 1$ is significant and for B, G, H, I only $J = 0$ is significant. A numerical example is $E^0_{110}/(\sqrt{3}E^1_{110}) = 9 \times 10^{-4}$.

3. Selection rule for l. If the spin-isospin part of the operator is even(odd) under the interchange or particle labels 2 and 3 then only matrix elements for which l is even(odd) are significant e.g. A requires $l =$ odd. This selection rule follows from the symmetry of the wavefunctions under interchange of particle labels.

4. A selection rule peculiar to the F type matrix elements is that F^1_{111} is zero by interchange of particle labels 1 and 2.

Further to the selection rules a rationalization of the matrix elements was possible by taking into account the long wavelength of the $W^\pm$ boson mediating the interaction, the low P-state probability ($< 0.2\%$) and the $\sim 9\%$ D-state probability in the trion wavefunctions. With regard to the first point we note that the isovector spectator point-particle range is about 1.7 fm. This implies that matrix elements with high values of λ are small and that a power expansion in y rapidly converges, e.g. the y^2 term in $j_0(Qy/3)$ contributes at the 3% level. The range of the pair coordinate x is of the order of the pion Compton wavelength, 1.4 fm, as can be seen from Fig. 1. This is expected because the exchange current operators pick out the spin and isospin dependence in the wavefunction which is mostly due to pion exchange. Matrix elements with the factor $j_f(Qx/2)$ will be small for large values of f.

Integrals of the densities are given in Table IV. An example of rationalization is to consider the ratios $D^1_{202}/D^1_{000} = 2 \times 10^{-1}$ and $D^1_{022}/D^1_{202} = 1 \times 10^{-2}$. We note that D^1_{000} receives contributions solely from SS overlap. D^1_{202} and D^1_{022} are dominated by SD overlap and are thus diminished due to the lower D-state probability by a factor $\sim \sqrt{(}0.09/0.91) =$

3×10^{-1} which explains the ratio of D^1_{202} and D^1_{000}. D^1_{022} is further suppressed due to the low momentum transfer in the process by the $j_2(Qy/3)$ factor[1] $\sim 3 \times 10^{-2}$. This explains why D^1_{022} is so much smaller than D^1_{202}.

For most local currents the leading multipoles plus those within one unit of angular momentum were included. This procedure neglects contributions at the 3% level. For the largest current (delta excitation) these 3% corrections were included.

The matrix elements ${}_yZ^J_{l\lambda L}$ and ${}_yZ^{K1J}_{l\lambda L}$ were neglected since we expect their contributions to be small compared to those of ${}_xZ^J_{l\lambda L}$ and ${}_xZ^{K1J}_{l\lambda L}$. They will be suppressed by about 15% due to angular momentum propensity rules. By parity we need an extra factor $\vec{x}$ or $\vec{y}$ to combine with ∇_y. In the case of $\vec{x}$ this yields $l = \lambda = 1$ and these elements are suppressed as can be seen in Table IV. In the case of $\vec{y}$ there will be suppression because of the $j_1(Qy/3)$ factor of about 15%.

The fact that we omit the non-local terms involving ∇_y implies that our estimate of the non-local terms has an inherent uncertainty of about 10-20%. It turns out that the non-local currents due to ∇_x contribute at the 10% level to the exchange currents and so the above neglect affects the results for the MEC at the 1-2% level and the results for the total current at less than the 0.5% level.

Each exchange current yields a contribution to one, (or more), of the current amplitudes and the general form is,

$$j = \int dx\, \rho(x)\, f(x) \tag{2.6}$$

where $\rho(x)$ is a nuclear density and $f(x)$ is a 'potential function' which depends on the meson which is exchanged, the overall coupling strength and also the momentum dependence of the current. The definitions of the various potential functions entering the calculation are given in appendix D.

The nuclear densities were calculated using wavefunctions found by the coupled rearrangement channel (CRC) method of Kameyama *et al.* [12]. The Faddeev components are expressed as sums of gaussians and one can find analytic expressions for the matrix element densities as functions of x, the pair coordinate. The densities were evaluated at either 14 points or in the case of the large matrix elements (first five of Table IV and the matrix elements with a derivative i.e. ${}_xZ^J_{l\lambda L}$), at 24 points with a higher density of points for $x < 1.5$ fm. The reason for calculating a density is to facilitate the calculation of matrix elements with different potential functions which necessity arises when meson coupling parameters and strong form factor cutoffs $\Lambda_\pi, \Lambda_\rho$ and Λ_a are varied.

The calculation of the local matrix elements was checked by comparing results for the trion isovector magnetic moment, μ_v, with those of Friar *et al.* [5]. In that work, wavefunctions for the triton were applied resulting from many NN potentials one of which was the AV14 potential: only exchange currents arising from π exchange were considered. With π exchange only, the expression for μ_v in our formalism is,

---

[1] Note that one-body currents have a $j_\lambda(2Qy/3)$ factor showing that the effective momentum transfer for exchange currents is half as much as for single-nucleon currents.

$$\mu_v = \lim_{Q\to 0}(-)\frac{m_p}{Q} j_x^{(1)} \quad \text{n.m.} \tag{2.7a}$$

$$= \mu_v^{\rm IA} + \mu_v^{\rm MEC} \tag{2.7b}$$

where,

$$\mu_v^{\rm IA} = \tfrac{1}{2}(1+\kappa^p-\kappa^n)[\boldsymbol{\sigma}]^{0,1} \tag{2.7c}$$

$$\mu_v^{\rm MEC} = \mu_v^{\rm pair} + \mu_v^{\pi} + \mu_v^{\Delta} \tag{2.7d}$$

and,

$$\begin{aligned}\mu_v^{\rm pair} = (-)\frac{m_p}{m_\pi} f_{\pi NN}^2 \Big\{ &\tfrac{1}{\sqrt{2}} D_{000}^1[\tfrac{x_\pi}{6} f_1] + \tfrac{1}{2} D_{202}^1[\tfrac{x_\pi}{6} f_1] + \tfrac{1}{\sqrt{6}} C_{111}^1[\tfrac{y_\pi}{9} f_1] \\ &- \tfrac{5}{\sqrt{24}} E_{111}^1[\tfrac{y_\pi}{9} f_1] - \tfrac{5}{\sqrt{8}} E_{110}^1[\tfrac{y_\pi}{9} f_1] \Big\}\end{aligned} \tag{2.7e}$$

$$\begin{aligned}\mu_v^{\pi} = (-)\frac{m_p}{m_\pi} f_{\pi NN}^2 \Big\{ &\tfrac{1}{\sqrt{2}} D_{000}^1[\tfrac{1}{3} d_3 - d_2] + \tfrac{1}{6} D_{202}^1[d_3] + \tfrac{1}{\sqrt{6}} C_{111}^1[\tfrac{y_\pi}{9}(d_5 - 5d_3/x_\pi)] \\ &- \tfrac{1}{\sqrt{30}} E_{111}^1[\tfrac{y_\pi}{9}(d_5 - 5d_3/x_\pi)] - \tfrac{1}{\sqrt{10}} E_{112}^1[\tfrac{y_\pi}{9}(d_5 - 5d_3/x_\pi)] \\ &- \tfrac{1}{\sqrt{15}} E_{312}^1[\tfrac{y_\pi}{9} d_5] - \sqrt{\tfrac{2}{15}} E_{313}^1[\tfrac{y_\pi}{9} d_5] \Big\}\end{aligned} \tag{2.7f}$$

$$\begin{aligned}\mu_v^{\Delta} = 2G_1 f_{\pi N\Delta} f_{\pi NN} \frac{4m_\pi m_p}{9M(M_\Delta - M)} \Big\{ &F_{000}^1[f_3 - f_2/2] + \tfrac{\sqrt{2}}{3} F_{202}^1[f_2] \\ &+ \tfrac{\sqrt{2}}{4} D_{000}^1[f_3 - f_2/3] - \tfrac{1}{12} D_{202}^1[f_2] \Big\}\end{aligned} \tag{2.7g}$$

where κ_p and κ_n are the proton and neutron anomalous magnetic moments and $\kappa_p - \kappa_n = 3.706$.

The calculation of Friar *et al.* [5] used a different potential function for μ_v^π arising from the propagator $\Delta_F^\pi(Q_2)\Delta_F^\pi(Q_3)F_{\pi NN}(Q_2)F_{\pi NN}(Q_3)$ which, although an intuitive choice, is inconsistent with the equation of continuity. To facilitate comparison we must replace $d_2 \to f_{25}, d_3 \to f_{26}$ and $d_5 \to f_{27}$ in Eq. (2.7f) (see appendix D for the definitions of functions f_i) where f_{25}, f_{26}, f_{27} correspond to the choice of propagator made in Ref. [5]. For the Δ-excitation graph we need to choose $f_{\pi N\Delta} = 6\sqrt{2}/5 f_{\pi NN}$ and $G_1 = 3\sqrt{2}/10(\mu_p - \mu_n) = 2.00$ so that our coefficients agree.

The comparison is shown in Table V. Our results for the exchange contributions are in overall agreement (case (b)) although the comparison is not exact because we have used a triton-helion overlap. Also shown are results with ^{3}H bra and ket wave vectors and τ_3^- replaced with $-\tau_3^z$ (case (a)) which corresponds exactly to the calculation of [5]. These results agree well. The agreement gives us confidence in our calculation of local matrix elements. We also give results for 8 and 22 channel wavefunctions from the AV14 potential with the Tuscon-Melbourne three-body force (cases (c) and (d)) which show the effect of adding extra channels to the Faddeev wavefunction. The effect is very small. Although a direct comparison of our results with [5] is not possible because a different coupling scheme was employed there (our wavefunctions employ Russell-Saunders LS coupling rather than jj) our 8 and their 5 channel wavefunctions have similar content and convergence of the binding energy requires 22 and 34 channels respectively. The extra channels change the pair, pion and delta contributions by less than 1% in our case whereas the difference in [5] is about 9%. This is a manifestation of the faster convergence obtained when using the CRC method: the projection of the potential onto partial waves is nearer to being complete for a given number of Faddeev component channels for the CRC method as compared to the method used in Ref. [5].

To check the calculation of the non-local matrix elements we used a Peterson type device [13]. The device follows from a simple identity for the matrix element of an operator $\mathcal{O}$ multiplied by the momentum operator $\hat{p}$ when the bra and ket vectors are equal. If,

$$M = \langle \psi \mid \mathcal{O}\hat{p} \mid \psi \rangle \tag{2.8}$$

then for $\mathcal{O}$ hermitian ($\mathcal{O}^\dagger = \mathcal{O}$),

$$\Im M = \frac{1}{2i} \langle \psi \mid [\mathcal{O}, \hat{p}] \mid \psi \rangle \tag{2.9}$$

and for $\mathcal{O}$ anti-hermitian ($\mathcal{O}^\dagger = -\mathcal{O}$),

$$\Re M = \frac{1}{2} \langle \psi \mid [\mathcal{O}, \hat{p}] \mid \psi \rangle . \tag{2.10}$$

Applying the above to the operator $\mathcal{O} = i\sigma_3 \cdot \vec{x}\, \tau_3$ we obtained,

$$\tfrac{3}{2}\, {}^{tt}F^{1}_{000} = -{}^{tt}_{x}F^{1}_{000} + \sqrt{2}\, {}^{tt}_{x}F^{1}_{202} + 3\, {}^{tt}_{x}F^{011}_{101} . \tag{2.11}$$

The ‘tt’ superscript indicates that the triton spin-space wavefunctions were used in both bra and ket and that $Q = 0$. Eq. (2.11) relates a local matrix element F^1_{000} to non-local matrix elements both *with* (${}_xF^1_{000}, {}_xF^1_{202}$) and *without* (${}_xF^{011}_{101}$) derivatives. The relation (2.11) was found to hold to within the precision[2] of the calculation and to 0.4% when the ket was replaced by a ^{3}He wavefunction. This deviation is first order in small differences between the ^{3}He and ^{3}H wavefunctions whereas the deviation given in equation (2.5) is second order which explains why the latter is smaller.

A further check of the calculation was made by calculating the Gamow-Teller matrix element, M(GT), which measures the axial current at zero momentum transfer and governs the β-decay of the triton. Our results are compared to those of Adam *et al.* [3] in Table VI. The calculation reported in Ref. [3] used axial currents which, except for the Δ-excitation currents, are equal to those used here and applied various wavefunctions and meson parameters (the values given in the table are for the Paris potential [14]). For the purposes of Table VI we have adopted the meson parameters given in Eq. (3.2) of Ref. [3]. However, because our hadronic form factors are monopole $F(Q^2) = [(\Lambda^2 - m^2)/(\Lambda^2 + Q^2)]^n$ with $n = 1$ and those used by Adam *et al.* had $n = \frac{1}{2}$, we applied equivalent values for Λ found by equating the slope of $F(Q^2)$ with respect to Q^2 at the on shell point $Q^2 = -m^2$. This procedure yielded,

---

[2] The expansion coefficients for the basis functions are know to a finite precision. By noting the largest contribution to the matrix element one can calculate the precision of the matrix element.

$$\Lambda_\pi(\text{monopole}) = 1.69 \text{ GeV} \leftrightarrow \Lambda_\pi(n = \tfrac{1}{2}) = 1.2 \text{ GeV} \tag{2.12a}$$

$$\Lambda_\rho(\text{monopole}) = 2.72 \text{ GeV} \leftrightarrow \Lambda_\rho(n = \tfrac{1}{2}) = 2.0 \text{ GeV}. \tag{2.12b}$$

Taking into account the different wavefunctions used the results agree quite well.

To check the calculation of the Δ-excitation currents we compared our results for M(GT) to those of Carlson *et al.* [15]. That calculation used wavefunctions found from the AV14 NN potential and the Urbana three-body force. Our wavefunction should therefore be only slightly different since the three-body force has only a small effect. To make the coupling coefficients the same we set $f^2_{\pi NN}/4\pi = 0.079$, $f^2_{\pi\Delta N}/4\pi = 0.2275$, $g_A(0) = -1.262$, $g^2_{\rho NN}/4\pi = 0.5$, $\kappa_V = 6.6$ and $G_1 = 3.06$. The pion and rho cutoffs were set to $\Lambda_\pi = 0.90$ GeV, $\Lambda_\rho = 1.35$ GeV which makes our potential functions agree exactly since Carlson *et al.* used monopole form factors. With these parameters we found that M(GT) received contributions +0.052 and –0.022 from the currents ANP4 and ANP5 respectively which agree well with the values reported in Table I of Ref. [15].

III. RESULTS

We precede the presentation of results with a discussion of our choices of parameters. The ranges used for the parameters which define the exchange currents are listed in Table VII. Our aim is to make a realistic estimate of the theoretical uncertainty and so we choose large ranges of reasonable values.

We took the ratio of the rho anomalous to normal coupling, $\kappa_{\rm V}$, to vary between 3.7 and 6.6. In the context of the hard-pion model, which combines vector meson dominance (VMD) with chiral symmetry, the value 3.7 is consistent as this is the VMD value. However, the Bonn meson exchange force model OBEPR [16] requires $\kappa_V = 6.6$. A similar criterion was applied to find the range of the ρNN coupling where the hard-pion model requires the KSRF [17] value $g^2_{\rho NN}/4\pi = 0.70$ whereas OBEPR favours a stronger coupling of $g^2_{\rho NN}/4\pi = 0.95$. The value of the $\rho N\Delta$ coupling, G_1, is taken from experimental data for the M1/E2 multipole ratio for photoproductions of pions [18]. The parameters ν and η reflect the off-shell ambiguity in the pion exchange potential. For consistency with the AV14 potential, which is a static potential, their values should be taken to be 1/2. Our exchange current APSPV expresses the difference between what would be obtained using pseudoscalar and pseudovector πNN coupling. Pseudoscalar coupling corresponds to $\lambda = 1$ and pseudovector coupling to $\lambda = 0$. It is not possible to achieve exact consistency of this current with the NN potential but the value $\lambda = 1/2$ is the most appropriate. We varied λ between 0 and 1. The value of $f^2_{\pi NN}/4\pi$ should be taken as 0.081 to be consistent with the AV14 potential. However, the range 0.075 - 0.081 was used to estimate the uncertainty due to $f_{\pi NN}$ where the low value comes from a recent Nijmegen analysis of NN scattering data [19].

The most influential parameters are the strong form factor cutoffs $\Lambda_\pi, \Lambda_\rho, \Lambda_a$ and the $\pi N\Delta$ coupling $f_{\pi N\Delta}$. The strong form factors affect the potential functions $f_i(x)$ entering the reduced matrix elements and in general reduce their strength at small x i.e. $x <\sim 1/\Lambda$. The value $\Lambda_M = m_M$ where $M = \pi, \rho$ or a_1 corresponds to complete cutoff. For example the current for Δ-excitation due to ρ exchange, ANP5, would be zero if the choice $\Lambda_\rho = m_\rho$ was made. We used the range $\Lambda_\pi = 1.0 - 1.5$ GeV which corresponds to a central value of 1.2 GeV with a 20% variation in $1/\Lambda_\pi$ either side. The values of Λ_ρ and Λ_a were then found by demanding consistency between the exchange current and the NN potential used to construct the wavefunction. The exchanges of π, ρ, a_1 yield isospin dependent spin-spin and tensor interactions (V_S and V_T) and it is these two components of the AV14 NN force which were fitted. The long range parts of V_S and V_T are fitted exactly provided the same pion coupling $f_{\pi NN}$ and pion mass are used. The short range part is affected by the strong form factors and the desired effect of the form factors is that the strength of the potential at short distance is reduced. Monopole form factors achieve this effect for V_T but for V_S an undesirable change in sign at small distance occurs. This can be traced back to the second derivative of the potential function arising from π, ρ or a_1 exchange. To illustrate this consider the π OBEP potential (see appendix E for further details).

$$V_T^\pi \sim F_\pi^{''} - \frac{F_\pi^{'}}{x_\pi} \tag{3.1a}$$

$$V_S^\pi \sim F_\pi^{''} + 2\frac{F_\pi^{'}}{x_\pi} \tag{3.1b}$$

where $F^{'} = dF/dx_\pi$. Fig. 2 shows $V_T^\pi, V_S^\pi, F_\pi^{'}$ and $F_\pi^{''}$ for $\Lambda_\pi \to \infty$ and $\Lambda_\pi = 1.2$ GeV. The function $F_\pi^{''}$ changes sign at $x_\pi \approx 0.16$ and we also have,

$$x_\pi F_\pi^{''} \to F_\pi^{'} \text{ as } x \to 0. \tag{3.2}$$

This explains why the combination of $F_\pi^{''}$ and $F_\pi^{'}$ in V_T does not change sign at small x despite containing $F_\pi^{''}$. The combination $(V_T - V_S)$ eliminates $F_\pi^{''}$. In order not to be sensitive to the short range part of $F_\pi^{''}$ we fitted Λ_ρ, Λ_a to V_T and $(V_T - V_S)$ where the latter combination eliminates $F_\pi^{''}$. *A posteriori* we noticed that the largest exchange currents are ANP4 for j_σ and VP1 for $j_x^{(1)}$. These currents have the form,

$$\Delta j_\sigma[\text{ANP4}] \sim \int dx [F_{202}^1(x) - \tfrac{1}{4} D_{202}^1(x)] \times j_0(Qx/2)\, V_T^\pi(x) \tag{3.3a}$$

$$\Delta j_x^{(1)}[\text{VP1}] \sim \int dx D_{000}^1(x) \times j_1(Qx/2)\, x_\pi [V_T^\pi(x) - V_S^\pi(x)] \tag{3.3b}$$

The above observation shows that the parts of the potential which are most important to fit well are V_T^π and $V_T^\pi - V_S^\pi$ in the ranges where $(F_{202}^1 - \frac{1}{4} D_{202}^1) j_0(Qx/2)$ and $D_{000}^1\, j_1(Qx/2) x_\pi$ are appreciable. The above considerations led to the following practical procedure. We minimized the function $f^{pq}(\Lambda_\rho, \Lambda_a)$ where,

$$f^{pq} = (I_T - I_T^0)^2 + (I_{TS} - I_{TS}^0)^2 \tag{3.4a}$$

and,

$$I_T = \int_0^\infty dx\, x^p\, V_T^{\text{OBEP}}(x) \tag{3.4b}$$

$$I_T^0 = \int_0^\infty dx\, x^p\, V_T^{\text{AV14}}(x) \tag{3.4c}$$

$$I_{TS} = \int_0^\infty dx\, x^q\, (V_T^{\rm OBEP}(x) - V_S^{\rm OBEP}(x)) \tag{3.4d}$$

$$I_{TS}^0 = \int_0^\infty dx\, x^q\, (V_T^{\rm AV14}(x) - V_S^{\rm AV14}(x)). \tag{3.4e}$$

The choice $(p,q) = (3,3)$ makes the integrand in I_T peak at $x = 1.6$ fm and the integrand in I_{TS} peak at 1.9 fm and gives the best matching of shape to the nuclear densities for ANP4 and VP1. Examples of fit values for Λ_ρ, Λ_a are given in Table VIII. We see that Λ_ρ is smaller when κ_V is larger as one would expect. The value of Λ_a is poorly constrained and apparently may vary between m_a and Λ_ρ.

To summarize, Λ_ρ and Λ_a were chosen to match the isospin dependent spin-spin and tensor potentials used to construct the wavefunction. They are functions of $\Lambda_\pi, f_{\pi NN}, g_{\rho NN}$ and κ_V and functionals of $V_T^{\rm AV14}$ and $V_S^{\rm AV14}$. This somewhat artificial procedure would be unnecessary if the wavefunctions were constructed using OBEP potentials found from the same lagrangian as the exchange currents were derived from. In that case $\Lambda_\pi, \Lambda_\rho$ and Λ_a would be fixed by the deuteron properties and NN scattering data. An alternative improvement which could be made is to choose a different type of form factor, the idea being to match the shape of V_T^{AV14} and V_S^{AV14} very closely.

There are four estimates of the $\pi N\Delta$ coupling $f_{\pi N\Delta}$. The simplest constituent quark model yields $f_{\pi N\Delta} = 6\sqrt{2}/5 f_{\pi NN}$ and hence $f_{\pi N\Delta}^2/4\pi = 0.23$. Dispersion theory yields $f_{\pi N\Delta}^2/4\pi = 0.29$ [20]. The Δ width of 120 MeV implies $f_{\pi N\Delta}^2/4\pi = 0.35$ [21]. The highest estimate is $f_{\pi N\Delta}^2/4\pi = 0.36$ which is the value implied by relation $f_{\pi N\Delta} = 3/\sqrt{2} f_{\pi NN}$ coming from the Skyrme-Soliton model with $1/N_c$ corrections [22]. We note that this model also yields $f_{\pi NN}^2/4\pi = 0.080$ and $g_A = -1.28$ which are in good agreement with experiment.

We take the range $f_{\pi N\Delta}^2/4\pi = 0.23$ - 0.36 reflecting the various models: there is a large uncertainty in the value of this parameter.

Our calculation does not treat the effect of the Δ-isobar explicitly i.e. there are no ΔNN components in the wavefunction. We were therefore unable to take into account direct coupling to Δ-isobars present in the nuclei or the indirect effect of the Δ-isobars on the coupling of the nucleons. These processes have been considered for the axial current at zero momentum transfer by Adam *et al.* [3]. The direct coupling contributes +0.030 to the Gamow-Teller matrix element, M(GT), and the indirect effect –0.021 [23]. These two effects compensate each other although their sum, +0.009, is not insignificant.

A further deficiency of the calculation is the static approximation for the propagator of a ΔN pair. Hajduk *et al.* have shown that this approximation is not valid and leads to an overestimate of the Δ-excitation current by a factor of 1.9 for both M(GT) and μ_V, [24, Table 1]. The reason for the overestimate is that $M_\Delta - M$ is a poor estimate for the energy of the $NN\Delta$ configuration minus the energy of the NNN configuration. This is due to the fact that Δ-excitation occurs only in total orbital angular momentum 2 channels: for these channels the kinetic energy is large which contradicts the zero value given to it in the static approximation.

To improve the static approximation we replaced $M_\Delta - M$ by $M_\Delta - M + \langle T\rangle$ where $\langle T\rangle$ is some average excess kinetic energy. The value $\langle T\rangle = 110$ MeV was used, chosen so that the contribution of static approximation Δ-excitation to M(GT) found in Ref. [24], 0.055, is converted to the exact value of 0.031 plus the contribution from the ΔNN components, 0.009, i.e.

$$\frac{M_\Delta - M}{M_\Delta - M + \langle T\rangle} \times 0.055 = 0.040 \tag{3.5}$$

This procedure corrects the contribution of the Δ-isobar at zero momentum transfer but the Q dependence of our Δ contribution is not correct. According to Fig. 3 of [24], we overestimate the Δ-excitation current for $Q < 4$ fm^{-1} although the error is small at $Q = 0.52$ fm^{-1} which is the momentum transfer for nuclear muon capture by ^{3}He.

Finally we list the values used for other constants entering the calculation. We have used the three-momentum transfer $Q = 103.22$ MeV, the energy transfer given by lepton kinematics $Q_0 = 2.44$ MeV, $m_\pi = 138.03$ MeV, $M_N = 939$ MeV, $M_\Delta = 1232$ MeV, $m_\rho = 770$ MeV, $m_\mu = 105.66$ MeV, $f_\pi = 92$ MeV, $g_A(0) = -1.257 \pm 0.003$, $g_V = 0.974 \pm 0.001$, $g_M = 3.576 \pm 0.001$, $g_A = -1.236 \pm 0.003$ (the values for g_V, g_M and g_A are at $q^2 = -0.954 m_\mu^2$).

Besides the uncertainty in the parameters, we need to take into account the fact that there are many possible realistic NN potentials. Wavefunctions derived from these potentials will yield different matrix elements according to the relative strengths of the different parts of the potential e.g. tensor interaction. To take this into account properly requires calculating the observables using wavefunctions derived from all the different potentials. We were not able to do this but we did estimate the 'model uncertainty' by varying the size of the dominant matrix element densities by a constant factor i.e. independent of x. The size of this factor was determined as described below.

The one-body currents are dominated by $[\mathbf{1}]^0$ and $[\boldsymbol{\sigma}]^{0,1}$. The variation in the value of $[\mathbf{1}]^0$ can be neglected since all models will agree at $Q = 0$ [3] and will have the same deviation from that value at low Q provided the isovector radius is reasonable. This condition will be satisfied for wavefunctions derived from realistic potentials which possess the correct binding energy because of scaling [25].

The above assertion was tested by calculating $[\mathbf{1}]^0$ at $Q = 103$ MeV with the AV14 and AV14+3BF 8 channel wavefunctions which have different binding energies. The bessel functions entering the matrix element can be expanded at small Q as,

$$j_0(2Qy/3) = 1 - Q^2y^2/54 + \dots \tag{3.6}$$

and so the change, Δ, in $[\mathbf{1}]^0$ as Q changes from zero to a small finite value is $Q^2 < y^2 > /54$ which scales as $1/E_B$. If we use the mean ^{3}He/^{3}H binding energy and the value $[\mathbf{1}]^0 = 0.851$ for the AV14+3BF wavefunctions then scaling implies,

$$\Delta(AV14) = 0.149 \times \frac{(8.34 + 7.67)}{(7.66 + 7.01)} = 0.163. \tag{3.7}$$

The above scaling argument predicts $[\mathbf{1}]^0 = 0.837$ for the AV14 wavefunctions which is close to the calculated value of 0.839: this result supports the argument that the model dependence in the value of $[\mathbf{1}]^0$ is small.

---

[3] The value is one minus a correction of the order of few $\times 10^{-4}$ due to isospin symmetry breaking

For $[\boldsymbol{\sigma}]^{0,1}$, however, differences do exist at $Q = 0$. The impulse approximation contributions μ_V^{IA} and $\mathrm{M(GT)}^{\mathrm{IA}}$ are both proportional to $[\boldsymbol{\sigma}]^{0,1}$ which allowed us to gauge the variation in $[\boldsymbol{\sigma}]^{0,1}$ due to the use of various wavefunctions. We used values for μ_V^{IA} reported in [5] for the Reid soft core (RSC), RSC+TM, RSC+Brazilian(BR), AV14, AV14+TM and AV14+BR potentials. Schiavilla *et al.* [26] report values for μ_V^{IA} for the AV14+Urbana VII and Urbana+Urbana VII potentials. The value of $[\boldsymbol{\sigma}]^{0,1}$ for the Paris potential was taken from the calculation of M(GT) reported in [3]. Calculations of M(GT) have also been performed for the Paris, super-soft core, AV14 and RSC potentials as reported in Ref. [27]. The range for $[\boldsymbol{\sigma}]^{0,1}$ from these sources is (–0.913) - (–0.932) and so in our calculation we varied $[\boldsymbol{\sigma}]^{0,1}$ by a factor ranging from 0.99 to 1.01. We did not include the large values of 0.937 and 0.943 reported in Refs. [3,27] for Bonn-type potentials in this analysis because of their very different nature. Bonn-type potentials will yield a peculiar balance between one-body and two-body currents: basically less two-body and more one-body because of their weak tensor force.

For the exchange currents the dominant matrix elements are D^1_{000}, F^1_{000}, D^1_{202} and F^1_{202} which enter into the Δ-excitation current and the pion pair (with PS coupling) or contact (with PV coupling) term. By studying the 34 channel entries of Tables IV and II of Ref. [5] we arrived at a common variation factor of 0.917 - 1.083 for D^1_{202} and F^1_{202} and 0.941 - 1.059 for D^1_{000} and F^1_{000}.

These variations due to 'model dependence' made significant contributions to the total uncertainty quoted as did the variations in $f_{\pi N\Delta}$ and Λ_π. The uncertainties in the observables were found by a Monte-Carlo analysis where the parameters were chosen randomly from their ranges with a flat probability distribution[4]. It was checked that the probability distribution for the observables was close to a normal distribution with the same mean and variance: one expects this because of the central limit theorem.

The final results are shown in Table IX and the uncertainties listed are one standard deviation. Also shown are results for the 8 channel wavefunction: there is little change in going from 8 to 22 channels for the wavefunctions used here although we did notice significant fractional changes in the value of the smaller matrix elements, in particular those dominated by total orbital angular momentum 1 states. We also include results found from the AV14 wavefunctions. The large difference in the rate is due to scaling rather than being a direct consequence of the three-body force. If the one-body currents are taken from the 22 channel AV14+3BF wavefunction and different wavefunctions used for the two-body currents, then the results shown in table X are obtained. These results are very similar to each other showing that the exchange currents are less sensitive to scaling than the one-body currents and that both one-body and two-body currents are insensitive to the increase in the number of channels in the CRC wavefunction.

In table XI we list the contributions of each current to the current amplitudes and effective form factors. The largest exchange current corrections are from the axial delta-excitation currents (ANP4-6) and the vector π-pair (contact) term (VP1). The agreement between the microscopic calculation and the EPM is very good except for $j_x^{(1)}$ and $j_x^{(2)}$ which differ by 7% and 11% respectively. Table XII shows the separate contributions of local and non-local currents.

---

[4] In the case of experimental uncertainties the range was taken as $\pm\sqrt{3}\sigma$

The dependencies of the observables on the nucleon pseudoscalar coupling g_P are shown in Fig. 3 and the sensitivies are listed in Table XIII. The dependence on g_P is similar to that on the trion pseudoscalar coupling F_P found in Ref. [1]. The rate is less sensitive to g_P than A_v which in turn is less sensitive than either A_t or A_Δ. The curves shown in Fig. 3 are well reproduced by parameterizing the effective couplings as follows and using Eqs. (3),(11),(12) and (13) of Ref. [1].

$$G_V = 0.835 \tag{3.8a}$$

$$G_P = 0.231 + 0.370r \tag{3.8b}$$

$$G_A = 1.300 \tag{3.8c}$$

where r is the ratio of g_P to its PCAC value.

Our result for μ_V is -2.52 ± 0.03 which agrees with the experimental value of –2.55. Our result for M(GT) is 0.977 ± 0.013 which also agrees with the experimental value of 0.961 ± 0.003.

IV. CONCLUSIONS

The calculation presented here used nucleonic and mesonic degrees of freedom to describe the charge changing weak nuclear current of the trion system at low momentum transfer. The two-nucleon component of the current is given by the π-MEC obtained from the hard-pion lagrangian of the $N\Delta\pi\rho A_1$ system. The nuclear system is described by wavefunctions derived by the coupled rearrangement channel method from the AV14 NN potential with Tuscon-Melbourne three-body force.

We first checked our numerics by calculating the trion isovector magnetic moment and the Gamow-Teller matrix element. The results of Table V and Table VI agree well with the results of Refs. [5] and [3], respectively.

Our analysis of the observables for reaction (1.1) shows that the main contribution comes from the space-like component of the current.

The potential π-MEC, connected with the nuclear OPEP via the nuclear continuity equation, is relatively well defined because the parameters of the OPEP are well known: every realistic potential should respect them. This statement is weakened by the fact that the AV14 potential is not of the OBEP type and the needed value of the cutoff Λ_π can be extracted only approximately (Table VII). The axial part of the potential MEC (entries 2-7 of Table XI) contributes significantly to G_P, while its contribution to G_A is only a minor one, because of a destructive interference of the individual contributions. The vector part of the potential MEC (lines 14-15 of Table XI) contribute both to G_A and G_P, with the prevailing contribution from the pair term VP1.

There are two sets of non-potential currents. One set is present only in the weak axial MEC and arises due to the interaction of the weak axial current with the $\pi\rho A_1$ system (currents ANP1-3). The contribution of these currents to the observables is only a minor one (lines 8-10 of Table XI). The other set of non-potential currents is formed by the Δ-excitation currents ANP4-6 and VNP1-2. The axial currents ANP4-6 contribute to G_A considerably (lines 11-13 of Table XI). This set of currents is much more model dependent and it is mainly responsible for the uncertainty of the calculation. It follows from the analysis of section III that the contribution from these currents is slightly overestimated due to the static limit in which these current are considered here.

One of our main goals is the analysis of the possibility of extraction of g_P. We have found that the rate is rather insensitive to it but the spin observables offer the opportunity of measuring g_P precisely (see Fig. 3). However, these kind of experiments are also more difficult to perform.

We presented the final results for the observables in Table IX. It can be seen that the microscopic calculations and the EPM predictions agree very well. In particular, our result for the transition rate for reaction (1.1) is,

$$\Gamma_0 = 1502 \pm 32\, s^{-1}\,. \tag{4.1}$$

Our estimate of the uncertainty in the calculation yields an error of ≈ 2 % in the value of the transition rate. The largest part of the uncertainty in Γ_0 comes from poor knowledge of $f_{\pi N\Delta}$. The value of Γ_0 Eq. (4.1) is in a good agreement with the preliminary results of the new precise measurement [28],

$$\Gamma_0^{\rm exp} = 1494 \pm 4\, s^{-1}\,. \tag{4.2}$$

Using this value we can compare (4.1) and (4.2) and conclude that

1. the structure of the space-like component of the weak axial π-MEC is well described at low momentum transfer within the framework of the phenomenological hard-pion method,
2. the value of the induced pseudoscalar constant g_P is,

$$\frac{g_P}{g_P^{\rm PCAC}} = 1.05 \pm 0.19 \tag{4.3}$$

and so the PCAC value of g_P is in rough agreement with the data as is the heavy baryon chiral perturbation theory value, $g_P^{CPT}/g_P^{\rm PCAC} = 1.01 \pm 0.02$ [29]. By $g_P^{\rm PCAC}$ we mean the value found from,

$$g_P^{\rm PCAC}(q^2) = \frac{2m_\mu M}{m_\pi^2 - q^2} g_A(q^2) \tag{4.4}$$

which yields $g_P^{\rm PCAC}(-0.954 m_\mu^2) = 8.12$. Let us note that the best measurement of ordinary muon capture by the proton [30] yields and uncertainty in g_P of 42% and combining various measurements reduces this to 22% [31].

The 0.19 uncertainty in g_P results almost entirely from the 2% theoretical uncertainty in the calculation of the rate. If the spin analyzing power A_v was measured and used to infer the value of $g_P/g_P^{\rm PCAC}$ then the lower limit on the uncertainty set by theory is 0.02.

REFERENCES

[1] J.G. Congleton and H.W. Fearing, Nucl. Phys. **A552**, 534 (1993).
[2] J. Adam Jr., E. Truhlík, S. Ciechanowicz and K. M. Schmitt, Nucl. Phys. **A507**, 675 (1990).
[3] J. Adam Jr., Ch. Hajduk, H. Henning, P. U. Sauer and E. Truhlík, Nucl. Phys. **A531**, 623 (1991).
[4] E. Truhlík and F. C. Khanna, Int. J. Mod. Phys. **A10**, 499 (1995).
[5] J.L.Friar *et al.*, Phys. Rev. **C37**, 2852 (1988).
E.L.Tomusiak *et al.*, Phys. Rev. **C32**, 2075 (1985).
[6] W. Struewe, Ch. Hajduk and P.U. Sauer, Nucl. Phys **A405**, 620 (1983).
[7] E. Hadjimichael and A. Barosso, Phys. Lett. **B47**, 103 (1973).
[8] M. Chemtob and M. Rho, Nucl. Phys. **A163**, 1 (1971).
[9] E. Truhlík and J. Adam Jr., Nucl. Phys. **A492**, 529 (1989).
[10] J.G. Congleton and E. Truhlík, in *Proc. of the 14th International Conference on Few-Body Problems in Physics*, edited by F.Gross, (Williamsburg, Virginia 1994), p761.
[11] Y.Wu, S.Ishikawa and T.Sasakawa, Phys. Rev. Lett. **64**, 1875 (1990).
[12] H.Kameyama, M.Kamimura and Y.Fukushima, Phys. Rev. **C40**, 974 (1989).
[13] E.A.Peterson, Phys. Rev. **167**, 971 (1968).
[14] M.Lacombe *et al.*, Phys. Rev. **C21**, 861 (1980).
[15] J. Carlson, D.O. Riska, R.Schiavilla and R.B. Wiringa, Phys. Rev **C44**, 619 (1991).
[16] R. Machleidt, K. Holinde and C. Elster, Phys. Rep. **149**, 1 (1987).
R. Machleidt, Adv. Nucl. Phys. **19**, 189 (1989).
[17] K. Kawarabayashi and M. Suzuki, Phys. Rev. Lett. **16**, 255 (1966).
Riazuddin and Fayyazuddin, Phys. Rev. **147**, 1071 (1966).
[18] R. Davidson, N.C. Mukhopadhyay and R. Wittmann, Phys. Rev. Lett. **56**, 804 (1986).
[19] V.G.J. Stoks, R.A.M. Klomp, C.P.F. Terheggen and J.J. de Swart, Phys. Rev. **C49**, 2950 (1994).
[20] J.Thakur and L.L.Foldy, Phys. Rev. **C8**, 1957 (1973).
[21] H.Sugawara and F. von Hippel, Phys. Rev. **172**, 1764 (1968).
[22] G.Holzwarth in *Baryons as Skyrme Solitons*, edited by G.Holzwarth, (World Scientific, Singapore 1993).
[23] H.Henning, private communication.
[24] Ch.Hajduk, P.U.Sauer and S.N.Yang, Nucl. Phys. **A405**, 605 (1983).
[25] J.L.Friar, B.F.Gibson, C.R.Chen and G.L.Payne, Phys. Lett. **161**, 241 (1985).
[26] R.Schiavilla, V.R.Pandharipande and D.O.Riska, Phys. Rev. **C40**, 2294 (1989).
[27] T-Y. Saito *et al.*, Phys. Lett. **242**, 12 (1990).
[28] A.A. Vorobyov *et al.*, to appear in *Proc. of the 15th European Conference on Few-Body Problems in Physics, 5-9 June*, (Peñiscola, Spain, 1995).
W. Prymas *et al.*, to appear in: *Proc. of Muon Catalyzed Fusion, μCF-95, 19-24 June*, (Dubna, Russia, 1995).
[29] V.Bernard, N.Kaiser and U.G.Meißner, Phys. Rev. **50**, 6899 (1994).
[30] G.Bardin *et al.*, Nucl. Phys. **A352**, 365 (1981).
[31] G.Bardin *et al.*, Phys. Lett. **B104**, 320 (1981).
[32] I.S. Towner, Phys. Rep. **155**, 263 (1987).
[33] E. Truhlík and K.-M. Schmitt, Few-Body Sys. **11**, 155 (1992).

ACKNOWLEDGMENTS

One of the authors (JGC) would like to acknowledge the support of the Institute for Theoretical Physics, Utrecht, the Netherlands where some of this work was performed. We are grateful to M.Kamimura who provided the coefficients for the nuclear wavefunctions. We would like to thank J.L.Friar and E.L.Tomusiak for providing us with additional information regarding the trion isovector magnetic moment calculation of Ref. [5] and J.Adam Jr. for useful discussions.

APPENDIX A: MOMENTUM SPACE CURRENTS

In this appendix we list the currents used in the calculation. They are written in their momentum space representation. Our conventions are that $g_A < 0$ and that the total current is the sum of the vector current j_V and the axial current j_A, not the vector current minus the axial current. The overall sign of the currents are consistent with the dominant one-body axial current,

$$j_A^a(1) = +g_A \vec{\sigma} \frac{\tau^a}{2}. \tag{A1}$$

The one-body currents are listed below and are consistent with the scheme used in [1]. Here, the initial and final momenta of nucleon i are written $\vec{p}$ and $\vec{p}\,'$ respectively and the Pauli spin matrices for nucleon i are written $\vec{\sigma}$.

$$\begin{aligned}\vec{j}_A^a = \frac{\tau^a}{2}\Big\{ & g_A\Big[\vec{\sigma}\Big(1 - \frac{(\vec{p}\,' + \vec{p})^2}{8M^2}\Big) + \frac{1}{4M^2}\Big(i\vec{p} \times \vec{p}\,' + \vec{p}\,'(\vec{p}\cdot\vec{\sigma}) + \vec{p}(\vec{p}\,'\cdot\vec{\sigma})\Big)\Big] \\ & + g_P \frac{\vec{Q}}{m_\mu}\Big[\frac{\vec{\sigma}\cdot\vec{p}}{2M}\Big(1 - \frac{3\vec{p}^{\,2}}{8M^2} - \frac{\vec{p}\,'^2}{8M^2}\Big) - \frac{\vec{\sigma}\cdot\vec{p}\,'}{2M}\Big(1 - \frac{\vec{p}^{\,2}}{8M^2} - \frac{3\vec{p}\,'^2}{8M^2}\Big)\Big]\Big\}\end{aligned} \tag{A2}$$

$$\begin{aligned}\rho_A^a = \frac{\tau^a}{2}\Big\{ & g_A \frac{\vec{\sigma}\cdot(\vec{p}\,' + \vec{p})}{2M} \\ & + g_P \frac{Q_0}{m_\mu}\Big[\frac{\vec{\sigma}\cdot\vec{p}}{2M}\Big(1 - \frac{3\vec{p}^{\,2}}{8M^2} - \frac{\vec{p}\,'^2}{8M^2}\Big) - \frac{\vec{\sigma}\cdot\vec{p}\,'}{2M}\Big(1 - \frac{\vec{p}^{\,2}}{8M^2} - \frac{3\vec{p}\,'^2}{8M^2}\Big)\Big\}\end{aligned} \tag{A3}$$

$$\vec{j}_V^a = \frac{\tau^a}{2}\Big\{g_V\Big[\frac{\vec{p} + \vec{p}\,'}{2M} + \frac{i\vec{\sigma}\times(\vec{p}\,' - \vec{p})}{2M}\Big] + g_M\Big[\frac{i\vec{\sigma}\times\vec{Q}}{2M} - \frac{Q_0}{2M}\Big(\frac{\vec{Q}}{2M} + \frac{i\vec{\sigma}\times(\vec{p}\,' + \vec{p})}{2M}\Big)\Big]\Big\} \tag{A4}$$

$$\rho_V^a = \frac{\tau^a}{2}\Big\{g_V\Big[1 - \frac{(\vec{p}\,' - \vec{p})^2}{8M^2} + \frac{i\vec{\sigma}\cdot(\vec{p}\,'\times\vec{p})}{4M^2}\Big] + g_M\Big[-\frac{(\vec{p}\,' - \vec{p})^2}{4M^2} + \frac{i\vec{\sigma}\cdot(\vec{p}\,'\times\vec{p})}{2M^2}\Big]\Big\} \tag{A5}$$

Now follow the two-body currents which have been labeled APi, ANPi, VPi or VNPi for the sake of reference. A(V) stands for axial-vector (vector) and P(NP) stands for potential (non-potential) current. The currents are written in terms of non-local momenta $\vec{P}_2, \vec{P}_3$ and local momenta $\vec{Q}_2, \vec{Q}_3$ defined by,

$$\vec{P}_2 = \vec{p}_2^{\,\prime} + \vec{p}_2 \tag{A6}$$

$$\vec{Q}_2 = \vec{p}_2^{\,\prime} - \vec{p}_2 \tag{A7}$$

$$\vec{P}_3 = \vec{p}_3^{\,\prime} + \vec{p}_3 \tag{A8}$$

$$\vec{Q}_3 = \vec{p}_3^{\,\prime} - \vec{p}_3 \tag{A9}$$

where $\vec{p_i}^{'}$, $(\vec{p_i})$ is the momentum of nucleon i in the final (initial) state. The currents appearing below are for the pair of particles labeled (23) and the isospin component $a \in \{x, y, z\}$ i.e. we have written here $j^a(23)$. The total current for muon capture is then $j^{x-iy}(12) + j^{x-iy}(21) + j^{x-iy}(23) + j^{x-iy}(32) + j^{x-iy}(31) + j^{x-iy}(13)$. Given the current $j(23)$ for particles 2 and 3, the matrix element of the other five other currents $j(32), j(12)\ldots$ are equal to that of $j(23)$ which follows from the symmetry of the wavefunctions under interchange of particle labels.

First we list the weak axial potential currents;
the sum of the a_1-pole pair term and the PCAC constraint term,

$$\begin{aligned}\vec{j}_A^{\,a,\mathrm{bare}}[\mathrm{AP1{+}AP7}] = \left(\frac{g}{2M}\right)^2 \frac{g_A}{2M} \Delta_F^{\pi}(Q_3) F_{\pi NN}^2(Q_3)(\vec{\sigma}_3 \cdot \vec{Q}_3)\Big\{&[\vec{Q} + i\vec{\sigma}_2 \times \vec{P}_2]\tau_3^a \\ &+[\vec{P}_2 + i\vec{\sigma}_2 \times \vec{Q}]i(\tau_2 \times \tau_3)^a\Big\}\end{aligned} \tag{A10}$$

where the total current is related to the bare current for this current and currents AP3,AP4 and APSPV by,[5]

$$\vec{j}_A^{\,a} = F_A(Q)F_{\pi NN}(Q)\vec{j}_A^{\,a,\mathrm{bare}} + F_{\pi NN}(Q)(1 - F_A(Q))\frac{\vec{Q}}{Q^2 - Q_0^2}(\vec{Q} \cdot \vec{j}_A^{\,a,\mathrm{bare}}), \tag{A11}$$

the π-pole pair term plus π-pole contact term,

$$\begin{aligned}\vec{j}_A^{\,a}[\mathrm{AP2{+}AP6}] = &\left(\frac{g}{2M}\right)^2 \frac{g_A}{4M}\left(\frac{2m_\pi^2}{Q^2 - Q_0^2 + m_\pi^2}\right) F_{\pi NN}(Q)\Delta_F^{\pi}(Q_3)F_{\pi NN}^2(Q_3)\vec{Q}\frac{(\vec{\sigma}_3 \cdot \vec{Q}_3)}{m_\pi^2} \\ &\times\Big\{[\vec{Q}^2 + \vec{Q}_3^2 + i\vec{\sigma}_2 \cdot (\vec{P}_2 \times \vec{Q}_2)]\tau_3^a \\ &+[(\vec{Q} \cdot \vec{P}_2) + 4(\vec{Q}_3 \cdot \vec{P}_2) - 3(\vec{Q}_3 \cdot \vec{P}_3) + 3i\vec{\sigma}_2 \cdot (\vec{Q} \times \vec{Q}_3)]i(\tau_2 \times \tau_3)^a\Big\}\end{aligned} \tag{A12}$$

the π-retardation term,

$$\begin{aligned}\vec{j}_A^{\,a,\mathrm{bare}}[\mathrm{AP3}] = -&\left(\frac{g}{2M}\right)^2 \frac{g_A}{4M}[\Delta_F^{\pi}(Q_3)]^2 F_{\pi NN}^2(Q_3)(\vec{\sigma}_3 \cdot \vec{Q}_3) \\ &\times\Big\{(1-\nu)(\vec{Q} \cdot \vec{Q}_3)[\vec{Q}_3\tau_3^a + i\vec{\sigma}_2 \times \vec{Q}_3 i(\tau_2 \times \tau_3)^a] \\ &+[(1-\nu)\vec{P}_2 \cdot \vec{Q}_3 + (1+\nu)\vec{P}_3 \cdot \vec{Q}_3][\vec{Q}_3 i(\vec{\tau}_2 \times \vec{\tau}_3)^a + i\sigma_2 \times Q_3\tau_3^a]\Big\}\end{aligned} \tag{A13}$$

the π-form factor term,

---

[5] In the calculation, the axial form factor $F_A(Q)$ was set to one so that the second term in Eq. (A11) yielded nothing. The correct value of $F_A(Q)$ is one minus 0.019.

$$\vec{j}_A^{a,\mathrm{bare}}[\mathrm{AP4}] = \left(\frac{g}{2M}\right)^2 \frac{g_A}{4M}\Delta_F^\pi(Q_3)\frac{d}{dQ_3^2}F_{\pi NN}^2(Q_3)$$
$$\times(\vec{\sigma}_3\cdot\vec{Q}_3)\Big\{(1-\eta)(\vec{Q}\cdot\vec{Q}_3)[\vec{Q}_3\tau_3^a + i\vec{\sigma}_2\times\vec{Q}_3 i(\tau_2\times\tau_3)^a]$$
$$+[(1-\eta)\vec{P}_2\cdot\vec{Q}_3 + (1+\eta)\vec{P}_3\cdot\vec{Q}_3][\vec{Q}_3 i(\vec{\tau}_2\times\vec{\tau}_3)^a + i\sigma_2\times Q_3\tau_3^a]\Big\}, \qquad \text{(A14)}$$

the current which measures the difference between exchange currents derived using pseudoscalar and pseudovector πN coupling,

$$\vec{j}_A^{a,\mathrm{bare}}[\mathrm{APSPV}] = -(1-\lambda)\left(\frac{g}{2M}\right)^2 \frac{g_A}{4M}\Delta_F^\pi(Q_3)F_{\pi NN}^2(Q_3)$$
$$\times\Big\{\Big[[\vec{P}_2 + i\vec{\sigma}_2\times\vec{Q}](\vec{\sigma}_3\cdot\vec{Q}_3) - \vec{Q}_3(\vec{\sigma}_3\cdot\vec{P}_3)\Big]i(\tau_2\times\tau_3)^a$$
$$+\Big[[\vec{Q} + i\vec{\sigma}_2\times\vec{P}_2](\vec{\sigma}_3\cdot\vec{Q}_3) - i\vec{\sigma}_2\times\vec{Q}_3(\vec{\sigma}_3\cdot\vec{P}_3)\Big]\tau_3^a\Big\}, \qquad \text{(A15)}$$

the a_1-pole contact terms, normal plus anomalous,

$$\vec{j}_A^{a,\mathrm{bare}}[\mathrm{AP5}] = -\left(\frac{g}{2M}\right)^2 \frac{1}{2g_A}\Delta_F^\pi(Q_3)F_{\pi NN}(Q_3)F_{\rho NN}(Q_2)$$
$$\times\frac{(\vec{\sigma}_3\cdot\vec{Q}_3)}{2M}\Big\{\vec{P}_2 + (1+\kappa_V)i\vec{\sigma}_2\times\vec{Q}_2\Big\}i(\tau_2\times\tau_3)^a \qquad \text{(A16)}$$

$$\rho_A^{a,\mathrm{bare}}[\mathrm{AP5}] = -\left(\frac{g}{2M}\right)^2 \frac{1}{2g_A}\Delta_F^\pi(Q_3)F_{\pi NN}(Q_3)F_{\rho NN}(Q_2)$$
$$\times(\vec{\sigma}_3\cdot\vec{Q}_3)\Big\{1 + \frac{(1+2\kappa_V)}{8M^2}[-\vec{Q}_2^2 + i\vec{\sigma}_2\cdot(\vec{Q}_2\times\vec{P}_2)]\Big\}i(\tau_2\times\tau_3)^a, \qquad \text{(A17)}$$

where the relationship between the total and bare current in this case is[6]

$$\vec{j}_{A\mu}^a = F_A(Q)F_{\pi NN}(Q)\vec{j}_{A\mu}^{a,\mathrm{bare}} + F_{\pi NN}(Q)(1-F_A(Q))\frac{Q_\mu}{Q^2-Q_0^2}(\vec{Q}\cdot\vec{j}_A^{a,\mathrm{bare}} - Q_0\rho_A^{a,\mathrm{bare}}). \qquad \text{(A18)}$$

Here follow the weak axial non–potential currents. They are;
the $a_1\rho\pi$ term,

$$\vec{j}_A^{a,\mathrm{bare}}[\mathrm{ANP1}] = -\left(\frac{g}{2M}\right)^2 \frac{1}{8Mg_A}\Delta_F^\rho(Q_2)\Delta_F^\pi(Q_3)F_{\rho NN}(Q_2)F_{\pi NN}(Q_3)(\vec{\sigma}_3\cdot\vec{Q}_3)$$
$$\times\Big\{\Big[\vec{P}_2 + (1+\kappa_V)i\vec{\sigma}_2\times\vec{Q}_2\Big]\Big[\vec{Q}_2\cdot(\vec{Q}_3-\vec{Q}_2) + \frac{\vec{P}_2\cdot\vec{Q}_2}{M^2}(\vec{P}_2\cdot\vec{Q}_2 - \vec{P}_3\cdot\vec{Q}_3)\Big]$$
$$+\vec{Q}_2\Big[\vec{Q}_3\cdot(\vec{P}_3-\vec{P}_2) - (1+\kappa_V)i\vec{\sigma}_2\cdot(\vec{Q}_2\times\vec{Q}_3)$$
$$+\frac{(1+2\kappa_V)}{8M^2}(\vec{P}_2\cdot\vec{Q}_2)[-\vec{Q}_2^2 + i\vec{\sigma}_2\cdot(\vec{Q}_2\times\vec{P}_2)]\Big]\Big\}i(\tau_2\times\tau_3)^a \qquad \text{(A19)}$$

---

[6] Again, the $F_A(Q) = 1$ approximation was made so that the second term in Eq. (A18) yielded nothing.

$$\begin{aligned}\rho_A^{a,\mathrm{bare}}[\mathrm{ANP1}] = &-\left(\frac{g}{2M}\right)^2 \frac{1}{4g_A}\Delta_F^\rho(Q_2)\Delta_F^\pi(Q_3)F_{\rho NN}(Q_2)F_{\pi NN}(Q_3)(\vec{\sigma}_3\cdot\vec{Q}_3)\\ &\times\Big\{\Big[\vec{Q}_2\cdot(\vec{Q}_3-\vec{Q}_2)+\frac{(\vec{Q}_2\cdot\vec{P}_2)^2}{4M^2}\Big]\Big[1+\frac{(1+2\kappa_V)}{8M^2}[-\vec{Q}_2^2+i\vec{\sigma}_2\cdot(\vec{Q}_2\times\vec{P}_2)]\Big]\\ &-\frac{(\vec{Q}_2\cdot\vec{P}_2)}{4M^2}[(\vec{Q}_2\cdot\vec{P}_2)+(1+\kappa_V)i\vec{\sigma}_2\cdot(\vec{Q}_2\times\vec{Q}_3)]\Big\}i(\tau_2\times\tau_3)^a\end{aligned}\tag{A20}$$

where the relationship between total and bare current is given by Eq. (A18),
the $\rho\pi$ term,

$$\begin{aligned}\vec{j}_A^a[\mathrm{ANP2}] = &-\left(\frac{g}{2M}\right)^2\frac{m_\rho^2}{4Mg_A}F_{\pi NN}(Q)\Delta_F^\rho(Q_2)\Delta_F^\pi(Q_3)F_{\rho NN}(Q_2)F_{\pi NN}(Q_3)i(\tau_2\times\tau_3)^a\\ &\times(\vec{\sigma}_3\cdot\vec{Q}_3)\Big\{\vec{P}_2+(1+\kappa_V)i\vec{\sigma}_2\times\vec{Q}_2\Big\}\end{aligned}\tag{A21}$$

$$\begin{aligned}\rho_A^a[\mathrm{ANP2}] = &-\left(\frac{g}{2M}\right)^2\frac{m_\rho^2}{2g_A}F_{\pi NN}(Q)\Delta_F^\rho(Q_2)\Delta_F^\pi(Q_3)F_{\rho NN}(Q_2)F_{\pi NN}(Q_3)i(\tau_2\times\tau_3)^a\\ &\times(\vec{\sigma}_3\cdot\vec{Q}_3)\Big\{1+\frac{(1+2\kappa_V)}{8M^2}[-\vec{Q}_2^2+i\vec{\sigma}_2\cdot(\vec{Q}_2\times\vec{P}_2)]\Big\},\end{aligned}\tag{A22}$$

the $\rho\pi\pi$ term,

$$\begin{aligned}\vec{j}_A^a[\mathrm{ANP3}] = &-\vec{Q}\left(\frac{g}{2M}\right)^2\frac{m_\rho^2}{2Mg_A^2}\Delta_F^\pi(Q)\Delta_F^\rho(Q_2)\Delta_F^\pi(Q_3)F_{\rho NN}(Q_2)F_{\pi NN}(Q_3)\\ &\times(\vec{\sigma}_3\cdot\vec{Q}_3)\Big\{\vec{Q}_3\cdot(\vec{P}_3-\vec{P}_2)-(1+\kappa_V)i\vec{\sigma}_2\cdot(\vec{Q}_2\times\vec{Q}_3)\\ &+(\vec{Q}_3\cdot\vec{P}_3)\frac{(1+2\kappa_V)}{8M^2}[-\vec{Q}_2^2+i\vec{\sigma}_2\cdot(\vec{Q}_2\times\vec{P}_2)]\Big\}i(\tau_2\times\tau_3)^a.\end{aligned}\tag{A23}$$

delta-excitation, π propagator,

$$\begin{aligned}\vec{j}_A^a[\mathrm{ANP4}] = &\, g_A\frac{f_{\pi N\Delta}^2}{m_\pi^2}\frac{4}{9(M_\Delta-M)}\Delta_F^\pi(Q_3)F_{\pi NN}^2(Q_3)\\ &\times(\vec{\sigma}_3\cdot\vec{Q}_3)\Big\{\vec{Q}_3\tau_3^a+\tfrac{1}{4}i(\vec{\sigma}_2\times\vec{Q}_3)i(\tau_2\times\tau_3)^a\Big\},\end{aligned}\tag{A24}$$

delta-excitation, ρ propagator,

$$\begin{aligned}\vec{j}_A^a[\mathrm{ANP5}] = &-\left(\frac{f_{\pi N\Delta}}{m_\pi}\right)\frac{(1+\kappa_V)}{2M^2}\frac{4G_1g_\rho^2f_\pi}{9(M_\Delta-M)}\Delta_F^\rho(Q_3)F_{\rho NN}^2(Q_3)\\ &\times\Big\{\vec{Q}_3\times(\vec{\sigma}_3\times\vec{Q}_3)\tau_3^a+\tfrac{1}{4}i\vec{\sigma}_2\times(\vec{Q}_3\times(\vec{\sigma}_3\times\vec{Q}_3))i(\tau_2\times\tau_3)^a\Big\},\end{aligned}\tag{A25}$$

delta-excitation, a_1 propagator,

$$\vec{j}_A^a[\mathrm{ANP6}] = \left(\frac{f_{\pi N\Delta}}{f_{\pi NN}}\right)^2 g_A^3g_\rho^2\frac{4}{9(M_\Delta-M)}\Delta_F^a(Q_3)F_{aNN}^2(Q_3)\Big\{\bar{\sigma}_3\tau_3^a+\tfrac{1}{4}i\vec{\sigma}_2\times\bar{\sigma}_3 i(\tau_2\times\tau_3)^a\Big\}\tag{A26}$$

where,

$$\bar{\sigma}_3 = \vec{\sigma}_3 + \frac{\vec{Q}_3(\vec{\sigma}_3 \cdot \vec{Q}_3)}{M_{a_1^2}}. \tag{A27}$$

Finally we list the weak vector currents. They are;
the π-pair term, (with PS coupling) or π-contact term (with PV coupling),

$$\vec{j}_V^a[\mathrm{VP1}] = -\left(\frac{f_{\pi NN}}{m_\pi}\right)^2 \Delta_F^\pi(Q_3) F_{\pi NN}^2(Q_3) \vec{\sigma}_2 (\vec{\sigma}_3 \cdot \vec{Q}_3) i(\tau_2 \times \tau_3)^a, \tag{A28}$$

the pion current,

$$\begin{aligned} \vec{j}_V^a[\mathrm{VP2}] = &+\left(\frac{f_{\pi NN}}{m_\pi}\right)^2 \vec{Q}_2(\vec{\sigma}_2 \cdot \vec{Q}_2)(\vec{\sigma}_3 \cdot \vec{Q}_3) i(\tau_2 \times \tau_3)^a \\ &\times \frac{1}{Q_2^2 - Q_3^2}\left[\Delta_F^\pi(Q_3) F_{\pi NN}^2(Q_3) - \Delta_F^\pi(Q_2) F_{\pi NN}^2(Q_2)\right], \end{aligned} \tag{A29}$$

delta-excitation, π propagator,

$$\begin{aligned} \vec{j}_V^a[\mathrm{VNP1}] = &-\frac{2G_1}{M}\frac{4 f_{\pi N\Delta} f_{\pi NN}}{9m_\pi^2(M_\Delta - M)} \Delta_F^\pi(Q_3) F_{\pi NN}^2(Q_3) \\ &\times (\vec{\sigma}_3 \cdot \vec{Q}_3) i\vec{Q} \times \Big\{\vec{Q}_3 \tau_3^a + \tfrac{1}{4} i(\vec{\sigma}_2 \times \vec{Q}_3) i(\tau_2 \times \tau_3)^a\Big\}, \end{aligned} \tag{A30}$$

delta-excitation, ρ propagator,

$$\begin{aligned} \vec{j}_V^a[\mathrm{VNP2}] = &-\frac{(1+\kappa_V)}{2M}\left(\frac{G_1}{M}\right)^2 \frac{4g_\rho^2}{9(M_\Delta - M)} \Delta_F^\rho(Q_3) F_{\rho NN}^2(Q_3) \\ &\times i\vec{Q} \times \Big\{\vec{Q}_3 \times (\vec{\sigma}_3 \times \vec{Q}_3) \tau_3^a + \tfrac{1}{4} i\vec{\sigma}_2 \times (\vec{Q}_3 \times (\vec{\sigma}_3 \times \vec{Q}_3)) i(\tau_2 \times \tau_3)^a\Big\}. \end{aligned} \tag{A31}$$

APPENDIX B: TRANSFORMATION INTO CONFIGURATION REPRESENTATION

Purely local currents of the form $f(Q_2, Q_3) g(Q_3)$ were transformed into configuration representation according to,

$$\tilde{\jmath}_{23}(\vec{x}, \vec{y}\,) = \exp[i\vec{Q} \cdot (\tfrac{\vec{x}}{2} - \tfrac{\vec{y}}{3})] \int \frac{d^3q}{(2\pi)^3} \exp[-i\vec{q} \cdot \vec{x}\,] \times f(\vec{Q} - \vec{q}, \vec{q}\,)\, g(\vec{q}\,) \tag{B1a}$$

$$= \exp[i\vec{Q} \cdot (\tfrac{\vec{x}}{2} - \tfrac{\vec{y}}{3}\,)] f(\vec{Q} - i\grave{\nabla}_x, i\grave{\nabla}_x) \tilde{g}(x) \tag{B1b}$$

where,

$$\vec{x} = \vec{r}_2 - \vec{r}_3 \tag{B2a}$$

$$\vec{y} = \vec{r} - \frac{1}{2}(\vec{r}_2 + \vec{r}_3) \tag{B2b}$$

$$\tilde{g}(x) = \int \frac{d^3q}{(2\pi)^3} \exp[-i\vec{q}\cdot\vec{x}]g(\vec{q}) \tag{B2c}$$

and $\grave{\nabla}_x$ is a derivative acting only on the function immediately to its right, in this case $\tilde{g}(x)$.

This process yields an operator in configuration space with a plane wave factor, a spin-space part made from $\vec{\sigma}_2, \vec{\sigma}_3$ and $\hat{x}$, an isospin part and a potential function which is a function of $x = \mid \vec{x} \mid$. As an example consider the vector current π pair term.

$$\vec{j}^a_V(\vec{Q}_2, \vec{Q}_3) = -\left(\frac{f_{\pi NN}}{m_\pi}\right)^2 i(\tau_2 \times \tau_3)^a \vec{\sigma}_2(\vec{\sigma}_3 \cdot \vec{Q}_3)\Delta^\pi_F(Q_3)F^2_{\pi NN}(Q_3) \tag{B3}$$

$$\Rightarrow \vec{\tilde{j}}^a_V(\vec{x}, \vec{y}\,) = +f^2_{\pi NN} \exp[i\vec{Q}\cdot(\tfrac{\vec{x}}{2} - \tfrac{\vec{y}}{3})]i(\tau_2 \times \tau_3)^a i\vec{\sigma}_2(\vec{\sigma}_3 \cdot \hat{x})f_1(x) \tag{B4}$$

The potential function in this case is $f_1(x)$, (see Fig. 4), the isospin operator is $i(\tau_2 \times \tau_3)^a$ and the plane wave factor is $\exp[i\vec{Q}\cdot(\vec{x}/2 - \vec{y}/3)]$.

Non-local currents $(\alpha\vec{P}_2 + \beta\vec{P}_3)f(\vec{Q}_2, \vec{Q}_3)g(\vec{Q}_3)$ were transformed to,

$$\begin{aligned}\tilde{j}_{23}(\vec{x}, \vec{y}\,) = \exp[i\vec{Q}\cdot(\tfrac{\vec{x}}{2} - \tfrac{\vec{y}}{3})]\{f(\vec{Q} - i\grave{\nabla}_x, i\grave{\nabla}_x)\tilde{g}(x)\\ \times[\alpha(-2i\nabla_x + i\nabla_y) + \beta(2i\nabla_x + i\nabla_y)] + [\alpha(\vec{Q} - i\grave{\nabla}_x) + \beta i\grave{\nabla}_x]f(\vec{Q} - i\grave{\nabla}_x, i\grave{\nabla}_x)\tilde{g}(x)\}\end{aligned} \tag{B5}$$

An example of this type of term is part of the AP1+AP7 current.

$$\vec{j}^a_A(\vec{Q}_2, \vec{Q}_3, \vec{P}_2, \vec{P}_3) = -\left(\frac{f_{\pi NN}}{m_\pi}\right)^2 \frac{g_A}{2M} i(\tau_2 \times \tau_3)^a \times \vec{P}_2(\vec{\sigma}_3 \cdot \vec{Q}_3)\Delta^\pi_F(Q_3)F^2_{\pi NN}(Q_3) \tag{B6}$$

$$\begin{aligned}\Rightarrow \tilde{j}^a_A(\vec{x}, \vec{y}) = -f^2_{\pi NN} g_A \frac{m_\pi}{2M} \exp[i\vec{Q}\cdot(\tfrac{\vec{x}}{2} - \tfrac{\vec{y}}{3})]i(\tau_2 \times \tau_3)^a \times \{i(\vec{\sigma}_3 \cdot \hat{x})f_1(x)[-2i\vec{\nabla}_x + i\vec{\nabla}_y]\\ + \frac{Q}{m_\pi}\hat{Q}i(\vec{\sigma}_3 \cdot \hat{x})f_1(x) - \hat{x}(\vec{\sigma}_3 \cdot \hat{x})f_2(x) + \vec{\sigma}_3 f_3(x)\}\end{aligned} \tag{B7}$$

The operator $\vec{\nabla}$ was written as the sum of a part with a derivative $\hat{x}\partial/\partial x$ and an angular part $\hat{\nabla}_x/x$ where,

$$\hat{\nabla}_x = \hat{\theta}_x \frac{\partial}{\partial\theta_x} + \frac{\hat{\phi}_x}{\sin\theta_x}\frac{\partial}{\partial\phi_x} \tag{B8}$$

APPENDIX C: LEADING CONTRIBUTIONS FROM EACH CURRENT

Here we write the contributions which were included from each current. The argument of the two-body matrix elements are potential functions f_i, (defined in appendix D), multiplied by either $j_0(Qx/2)$ which is suppressed for succinctness or $j_i(i \neq 0)$ which is then written, e.g. ${}_xB^1_{000}[f_1]$ means,

$$\langle\, {}^3\mathrm{H} \,||\, 12/\sqrt{3}[4\pi\mathcal{Y}^0_{00}(\hat{x}\hat{y}) \otimes S_0(\vec{\sigma}_2,\vec{\sigma}_3)]_1 i(\tau_2 \times \tau_3)^- f_1(x) j_0(Qx/2) j_0(Qy/3)\frac{\partial}{\partial x_\pi} \,||\, {}^3\mathrm{He}\,\rangle \tag{C1}$$

and $F^1_{112}[j_2 f_2]$ means,

$$\langle\, {}^3\mathrm{H} \,||\, 12/\sqrt{3}[4\pi\mathcal{Y}^2_{11}(\hat{x}\hat{y}) \otimes \vec{\sigma}_3]_1 \tau_3^- f_2(x) j_2(Qx/2) j_1(Qy/3) \,||\, {}^3\mathrm{He}\,\rangle. \tag{C2}$$

The one-body matrix elements $[\mathbf{1}]^0$, $[\boldsymbol{\sigma}]^\pm$ and $[\boldsymbol{\sigma}]^{l,1}$ are defined by Eqs. (47-50) of [1].

One-body current

$$\Delta\rho_0 = \Big[g_V\Big(1 - \frac{Q^2}{8M^2}\Big) - g_M\frac{Q^2}{4M^2}\Big][\mathbf{1}]^0 \tag{C3}$$

$$\Delta\rho_1 = -\frac{Q}{2M}\Big[-\frac{g_A}{3} + g_P\frac{q^0}{m_\mu}\Big(1 - \frac{Q^2}{24M^2}\Big)\Big][\sigma]^+ \tag{C4}$$

$$\Delta j_Q = \frac{Q}{2M}\Big[\frac{g_V}{3} - g_M\frac{q^0}{2M}\Big][\mathbf{1}]^0 \tag{C5}$$

$$\Delta j_x^{(1)} = -\frac{Q}{2M}\Big[g_V + g_M\Big(1 - \frac{q^0}{6M}\Big)\Big][\boldsymbol{\sigma}]^- \tag{C6}$$

$$\Delta j_\sigma = g_A\Big(1 + \frac{Q^2}{24M^2}\Big)[\boldsymbol{\sigma}]^{0,1} - \frac{1}{3}\frac{Q}{2M}\Big[g_A\frac{Q}{3M} + g_P\frac{Q}{m_\mu}\Big(1 - \frac{Q^2}{24M^2}\Big)\Big][\boldsymbol{\sigma}]^+ \tag{C7}$$

$$\Delta j_x^{(2)} = \frac{3}{\sqrt{2}}g_A\Big(1 + \frac{Q^2}{24M^2}\Big)[\boldsymbol{\sigma}]^{2,1} - \frac{Q}{2M}\Big[g_A\frac{Q}{3M} + g_P\frac{Q}{m_\mu}\Big(1 - \frac{Q^2}{24M^2}\Big)\Big][\boldsymbol{\sigma}]^+ \tag{C8}$$

AP1 + AP7

$$\begin{aligned}\Delta j_\sigma = -g_A f^2_{\pi NN} F_{\pi NN}(Q)\frac{m_\pi}{M} \times \Big\{&\tfrac{1}{3}{}_xB^1_{000}[f_1] - \tfrac{\sqrt{2}}{3}{}_xB^1_{202}[f_1] + \tfrac{\sqrt{2}}{3}{}_xH^1_{000}[f_1] + \tfrac{1}{3}{}_xH^1_{202}[f_1] \\ &+ \tfrac{1}{\sqrt{3}}{}_xI^1_{202}[f_1] -{}_x B^{011}_{101}[f_1] - \sqrt{\tfrac{2}{9}}{}_xG^{111}_{101}[f_1] - \sqrt{\tfrac{2}{3}}{}_xH^{111}_{101}[f_1] - \sqrt{\tfrac{10}{9}}{}_xI^{111}_{101}[f_1]\Big\}\end{aligned} \tag{C9}$$

AP2+AP6

$$\begin{aligned}\Delta j_x^{(2)} = 3\Delta j_\sigma = -g_A f^2_{\pi NN} F_{\pi NN}(Q)&\frac{2m_\pi^2}{(Q^2 - Q_0^2 + m_\pi^2)}\frac{Q}{2M}\frac{Q}{m_\pi} \\ &\times\Big\{-\tfrac{1}{\sqrt{2}}D^1_{000}[f_2 - 3f_3] - \tfrac{1}{2}D^1_{202}[f_2] + \tfrac{1}{3}{}_xB^1_{000}[f_1] - \tfrac{\sqrt{2}}{3}{}_xB^1_{202}[f_1] + \tfrac{\sqrt{2}}{3}{}_xH^1_{000}[f_1] \\ &+ \tfrac{1}{3}{}_xH^1_{202}[f_1] + \tfrac{1}{\sqrt{3}}{}_xI^1_{202}[f_1] -{}_x B^{011}_{101}[f_1] - \sqrt{\tfrac{2}{9}}{}_xG^{111}_{101}[f_1] - \sqrt{\tfrac{2}{3}}{}_xH^{111}_{101}[f_1] \\ &- \sqrt{\tfrac{10}{9}}{}_xI^{111}_{101}[f_1]\Big\}\end{aligned} \tag{C10}$$

AP3

$$\begin{aligned}\Delta j_\sigma = -\nu g_A f_{\pi NN}^2 F_{\pi NN}(Q)\frac{m_\pi}{M} \times \Big\{ & \tfrac{1}{3}{}_xB^1_{000}[5f_{20}-f_{19}] - \tfrac{\sqrt{2}}{3}{}_xB^1_{202}[2f_{20}-f_{19}] \\ & + \tfrac{\sqrt{2}}{3}{}_xH^1_{000}[5f_{20}-f_{19}] + \tfrac{1}{3}{}_xH^1_{202}[2f_{20}-f_{19}] + \tfrac{1}{\sqrt{3}}{}_xI^1_{202}[2f_{20}-f_{19}] - \tfrac{4}{3}{}_xB^{011}_{101}[f_{20}] \\ & + \tfrac{1}{\sqrt{3}}{}_xB^{111}_{101}[f_{20}] - \tfrac{\sqrt{5}}{3}{}_xB^{211}_{101}[f_{20}] + \tfrac{\sqrt{2}}{3}{}_xH^{011}_{101}[f_{20}] - \sqrt{\tfrac{3}{2}}{}_xH^{111}_{101}[f_{20}] \\ & - \sqrt{\tfrac{5}{18}}{}_xH^{211}_{101}[f_{20}] - \sqrt{\tfrac{5}{2}}{}_xI^{111}_{101}[f_{20}] + \sqrt{\tfrac{5}{6}}{}_xI^{211}_{101}[f_{20}]\Big\} \end{aligned} \tag{C11}$$

AP4 the same as for AP3 with

$$\begin{aligned} \nu &\to -2\eta \\ f_{19} &\to f_{21} \\ f_{20} &\to f_{22} \end{aligned} \tag{C12}$$

APSPV

$$\begin{aligned}\Delta j_\sigma = -(1-\lambda) g_A f_{\pi NN}^2 F_{\pi NN}(Q)\frac{m_\pi}{M} \times \Big\{ & \tfrac{-1}{3}{}_xB^1_{000}[f_1] + \tfrac{\sqrt{2}}{3}{}_xB^1_{202}[f_1] - \tfrac{\sqrt{2}}{3}{}_xH^1_{000}[f_1] \\ & - \tfrac{1}{3}{}_xH^1_{202}[f_1] - \tfrac{1}{\sqrt{3}}{}_xI^1_{202}[f_1] + \tfrac{2}{3}{}_xB^{011}_{101}[f_1] - \tfrac{1}{2\sqrt{3}}{}_xB^{111}_{101}[f_1] \\ & + \sqrt{\tfrac{5}{36}}{}_xB^{211}_{101}[f_1] - \sqrt{\tfrac{2}{36}}{}_xH^{011}_{101}[f_1] + \sqrt{\tfrac{3}{8}}{}_xH^{111}_{101}[f_1] \\ & + \sqrt{\tfrac{5}{72}}{}_xH^{211}_{101}[f_1] + \sqrt{\tfrac{5}{8}}{}_xI^{111}_{101}[f_1] - \sqrt{\tfrac{5}{24}}{}_xI^{211}_{101}[f_1]\Big\} \end{aligned} \tag{C13}$$

AP5

$$\begin{aligned}\Delta j_\sigma = -\frac{f_{\pi NN}^2}{g_A} F_{\pi NN}(Q)\frac{m_\pi}{2M} \times \Big\{ & \frac{(1+\kappa_V)}{2}\Big[\sqrt{2}D^1_{000}[f_5/3-f_6] + \tfrac{1}{3}D^1_{202}[f_5]\Big] \\ & + \Big[-\tfrac{1}{3}{}_xB^1_{000}[f_4] + \tfrac{\sqrt{2}}{3}{}_xB^1_{202}[f_4] +{}_x B^{111}_{101}[f_4]\Big]\Big\} \end{aligned} \tag{C14}$$

$$\Delta\rho_1 = G_3\Big\{\tfrac{\sqrt{2}}{3}{}_xD^1_{000}[f_4] + \tfrac{1}{3}{}_xD^1_{202}[f_4] - \sqrt{\tfrac{2}{3}}{}_xD^{111}_{101}[f_4]\Big\} \tag{C15}$$

where,

$$G_3 = (-)\frac{f_{\pi NN}^2}{g_A}\frac{m_\pi Q}{8M^2}(1+2\kappa_V)F_{\pi NN}(Q). \tag{C16}$$

ANP1

$$\begin{aligned}\Delta j_\sigma = -\frac{f_{\pi NN}^2}{g_A}\frac{m_\pi^2}{2Mm_\rho} \times \Big\{ & \frac{(1+\kappa_V)}{2}\Big[\sqrt{2}D^1_{000}[f_{15}/3 - f_{16} - \tfrac{7}{6}(\tfrac{Q}{m_\pi})^2(f_{12}/3 - f_{13})] \\ & + \tfrac{1}{3}D^1_{202}[f_{15} - \tfrac{7}{6}(\tfrac{Q}{m_\pi})^2 f_{12}]\Big] + \tfrac{1}{3}{}_xB^1_{000}[x_\pi f_{16} + 5f_{18} - f_{17} - \tfrac{1}{2}(\tfrac{Q}{m_\pi})^2 f_{11}] \\ & - \tfrac{\sqrt{2}}{3}{}_xB^1_{202}[x_\pi f_{16} + 2f_{18} - f_{17} - \tfrac{1}{2}(\tfrac{Q}{m_\pi})^2 f_{11}] \\ & -{}_xB^{011}_{101}[x_\pi f_{16} + \tfrac{4}{3}f_{18} - \tfrac{1}{2}(\tfrac{Q}{m_\pi})^2 f_{11}] + \tfrac{1}{\sqrt{3}}{}_xB^{111}_{101}[f_{18}] - \tfrac{\sqrt{5}}{3}{}_xB^{211}_{101}[f_{18}]\Big\} \end{aligned} \tag{C17}$$

$$\Delta j_x^{(2)} = -\frac{f_{\pi NN}^2}{g_A}(1+\kappa_V)\frac{Q^2}{16Mm_\rho} \times \Big\{\sqrt{2}D^1_{000}[f_{12}/3 - f_{13}] + \tfrac{1}{3}D^1_{202}[f_{12}]\Big\} \tag{C18}$$

$$
\begin{aligned}
\Delta\rho_1 = {} & (-)G_3\Big\{\tfrac{\sqrt{2}}{3}\,{}_xD^{1}_{000}[f_4] + \tfrac{1}{3}\,{}_xD^{1}_{202}[f_4] - \sqrt{\tfrac{2}{3}}\,{}_xD^{111}_{101}[f_4]\Big\} \\
& +G_3\frac{m_\rho}{m_\pi}\Big(1+\frac{Q^2}{2m_\rho^2}\Big)\Big\{\tfrac{\sqrt{2}}{3}\,{}_xD^{1}_{000}[f_{11}] + \tfrac{1}{3}\,{}_xD^{1}_{202}[f_{11}] - \sqrt{\tfrac{2}{3}}\,{}_xD^{111}_{101}[f_{11}]\Big\} \\
& +G_3\frac{m_\pi}{2m_\rho}\Big\{+{}_xD^{1}_{202}[f_{18}] - \tfrac{1}{\sqrt{6}}\,{}_xD^{011}_{101}[f_{18}] + \tfrac{1}{\sqrt{10}}\,{}_xD^{111}_{101}[f_{18}] - \tfrac{1}{\sqrt{15}}\,{}_xD^{211}_{101}[f_{18}]\Big\} \\
& +\frac{1+\kappa_V}{1+2\kappa_V}G_3\frac{m_\pi}{m_\rho}\Big\{{}_xD^{1}_{000}[5f_{18}-f_{17}] + \tfrac{1}{3}\,{}_xD^{1}_{202}[2f_{18}-f_{17}] + \tfrac{\sqrt{2}}{3}\,{}_xD^{011}_{101}[f_{18}] \\
& -\sqrt{\tfrac{3}{2}}\,{}_xD^{111}_{101}[f_{18}] - \tfrac{1}{3}\sqrt{\tfrac{5}{2}}\,{}_xD^{211}_{101}[f_{18}]\Big\} \\
& -\frac{1+\kappa_V}{1+2\kappa_V}G_3\frac{m_\rho}{2m_\pi}\Big\{\tfrac{\sqrt{2}}{3}\,{}_xD^{1}_{000}[3f_{13}-f_{12}-\tfrac{m_\pi}{m_\rho}(3f_6-f_5)] - \tfrac{1}{3}\,{}_xD^{1}_{202}[f_{12}-\tfrac{m_\pi}{m_\rho}f_5]\Big\} \qquad \text{(C19)}
\end{aligned}
$$

ANP2

$$
\begin{aligned}
\Delta j_\sigma = {} & -\frac{f^2_{\pi NN}}{g_A}\frac{(1+\kappa_V)m_\rho}{4M}F_{\pi NN}(Q)\times\Big\{\sqrt{2}D^{1}_{000}[f_{12}/3-f_{13}] + \tfrac{1}{3}D^{1}_{202}[f_{12}]\Big\} \\
& -\frac{f^2_{\pi NN}}{g_A}\frac{m_\rho}{2M}F_{\pi NN}(Q)\times\Big\{-\tfrac{1}{3}\,{}_xB^{1}_{000}[f_{11}] + \tfrac{\sqrt{2}}{3}\,{}_xB^{1}_{202}[f_{11}] +{}_x B^{011}_{101}[f_{11}]\Big\} \qquad \text{(C20)}
\end{aligned}
$$

$$
\Delta\rho_1 = G_3\frac{m_\rho}{m_\pi}\Big\{\tfrac{\sqrt{2}}{3}\,{}_xD^{1}_{000}[f_{11}] + \tfrac{1}{3}\,{}_xD^{1}_{202}[f_{11}] - \sqrt{\tfrac{2}{3}}\,{}_xD^{111}_{101}[f_{11}] \qquad \text{(C21)}
$$

ANP3

$$
\begin{aligned}
\Delta j^{(2)}_x = 3\Delta j_\sigma = {} & -\left(\frac{f_{\pi NN}}{g_A}\right)^2\frac{(1+\kappa_V)m_\rho Q^2}{2M(m_\pi^2-Q_0^2+Q^2)}\times\Big\{\sqrt{2}D^{1}_{000}[f_{12}/3-f_{13}] + 1/3D^{1}_{202}[f_{12}]\Big\} \\
& -\left(\frac{f_{\pi NN}}{g_A}\right)^2\left(\frac{m_\pi}{M}\right)^2\ \frac{(1+2\kappa_V)m_\rho Q^2}{4M(m_\pi^2-Q_0^2+Q^2)}\times\Big\{\tfrac{1}{3}\,{}_xB^{1}_{000}[f_{17}-5f_{18}] \\
& +\tfrac{\sqrt{2}}{3}\,{}_xB^{1}_{202}[2f_{18}-f_{17}] + \tfrac{4}{3}\,{}_xB^{011}_{101}[f_{18}] - \tfrac{1}{\sqrt{3}}\,{}_xB^{111}_{101}[f_{18}] + \tfrac{\sqrt{5}}{3}\,{}_xB^{211}_{101}[f_{18}]\Big\} \qquad \text{(C22)}
\end{aligned}
$$

ANP4

$$
\begin{aligned}
\Delta j_\sigma = {} & g_A f^2_{\pi N\Delta}\frac{4m_\pi}{9(M_\Delta-M)}\times\Big\{F^{1}_{000}[f_3-f_2/3] + \tfrac{\sqrt{2}}{3}F^{1}_{202}[f_2] \\
& +\tfrac{\sqrt{2}}{4}D^{1}_{000}[f_3-f_2/3] - \tfrac{1}{12}D^{1}_{202}[f_2]\Big\} \qquad \text{(C23)}
\end{aligned}
$$

Higher order terms for ANP4

$$
\begin{aligned}
\Delta j^{(2)}_x = {} & g_A f^2_{\pi N\Delta}\frac{4m_\pi}{9(M_\Delta-M)}\times\Big\{F^{1}_{000}[j_2f_2] - \tfrac{3}{\sqrt{2}}F^{1}_{202}[j_2(2f_2/3-f_3)] - \tfrac{3}{\sqrt{2}}F^{1}_{022}[j_0(f_2/3-f_3)] \\
& +\tfrac{2\sqrt{3}}{5}F^{1}_{110}[j_1f_2] + \sqrt{\tfrac{27}{5}}F^{1}_{110}[j_1(17f_2/30-f_3)] + \tfrac{1}{\sqrt{5}}F^{1}_{220}[j_0f_2] + \tfrac{3}{2\sqrt{5}}F^{1}_{221}[j_0f_2] \\
& +\sqrt{\tfrac{7}{20}}F^{1}_{222}[j_0f_2] - \tfrac{1}{4\sqrt{2}}D^{1}_{000}[j_2f_2] - \tfrac{3}{4}D^{1}_{202}[j_2(f_2/6-f_3)] - \tfrac{3}{4}D^{1}_{022}[j_0(f_2/3-f_3)] \\
& +\tfrac{9}{40}\sqrt{\tfrac{3}{10}}E^{1}_{111}[j_1f_2] + \tfrac{21}{40}\sqrt{\tfrac{1}{10}}E^{1}_{110}[j_1f_2]\Big\} \qquad \text{(C24)}
\end{aligned}
$$

$$\Delta j_\sigma = g_A f^2_{\pi N \Delta} \frac{4 m_\pi}{9(M_\Delta - M)} \times \Big\{ \sqrt{3} F^1_{110}[j_1(f_2/3 - f_3)] + \sqrt{\tfrac{4}{15}} F^1_{112}[j_1 f_2] \\ - \sqrt{\tfrac{1}{40}} E^1_{112}[j_1 f_2] \Big\} \tag{C25}$$

ANP5

$$\Delta j_\sigma = f_{\pi N \Delta} \frac{2 G_1 g^2_\rho (1 + \kappa_V) f_\pi}{9(M_\Delta - M)} \left(\frac{m_\pi}{M}\right)^2 \times \Big\{ F^1_{000}[f_7 - f_8/3] + \tfrac{\sqrt{2}}{3} F^1_{202}[f_8] \\ + \tfrac{\sqrt{2}}{4} D^1_{000}[f_7 - f_8/3] - \tfrac{1}{12} D^1_{202}[f_8] \Big\} \tag{C26}$$

ANP6

$$\Delta j_\sigma = \left(\frac{f_{\pi N \Delta}}{f_{\pi N N}}\right)^2 g^2_\rho g^3_A \frac{4 m^3_\pi}{9 m^2_a (M_\Delta - M)} \times \Big\{ F^1_{000}[F_8 + f_{24} - f_{23}/3] + \tfrac{\sqrt{2}}{3} F^1_{202}[f_{23}] \\ + \tfrac{\sqrt{2}}{4} D^1_{000}[F_8 + f_{24} - f_{23}/3] - \tfrac{1}{12} D^1_{202}[f_{23}] \Big\} \tag{C27}$$

VP1

$$\Delta j^{(1)}_x = f^2_{\pi N N} \times \Big\{ \tfrac{1}{\sqrt{2}} D^1_{000}[j_1 f_1] + \tfrac{1}{2} D^1_{202}[j_1 f_1] \\ + \tfrac{1}{\sqrt{6}} C^1_{111}[j_0 f_1] - \sqrt{\tfrac{5}{24}} E^1_{111}[j_0 f_1] - \sqrt{\tfrac{5}{8}} E^1_{110}[j_0 f_1] \Big\} \tag{C28}$$

VP2

$$\Delta j^{(1)}_x = f^2_{\pi N N} \frac{Q}{m_\pi} \Big\{ \tfrac{1}{\sqrt{2}} D^1_{000}[e_3/3 - e_2] + \tfrac{1}{6} D^1_{202}[e_3] \Big\} \tag{C29}$$

VNP1

$$\Delta j^{(1)}_x = - f_{\pi N \Delta} f_{\pi N N} \frac{8 G_1 m_\pi Q}{9 M (M_\Delta - M)} \times \Big\{ F^1_{000}[f_3 - f_2/3] + \tfrac{\sqrt{2}}{3} F^1_{202}[f_2] \\ + \tfrac{\sqrt{2}}{4} D^1_{000}[f_3 - f_2/3] - \tfrac{1}{12} D^1_{202}[f_2] \Big\} \tag{C30}$$

VNP2

$$\Delta j^{(1)}_x = \frac{2 G^2_1 g^2_\rho (1 + \kappa_V)\, m_\pi}{9(M_\Delta - M)} \left(\frac{m_\pi}{M}\right)^2 \frac{Q}{M} \times \Big\{ F^1_{000}[f_7 - f_8/3] + \tfrac{\sqrt{2}}{3} F^1_{202}[f_8] \\ + \tfrac{\sqrt{2}}{4} D^1_{000}[f_7 - f_8/3] - \tfrac{1}{12} D^1_{202}[f_8] \Big\} \tag{C31}$$

APPENDIX D: DEFINITION OF POTENTIAL FUNCTIONS

Here we define the potential functions f_i. They are derivatives of root potential functions F_i, e.g. $f_1 = -dF_1/dx_\pi, f_2 = d^2 F_1/dx^2_\pi - 1/x_\pi dF_1/dx_\pi$. We first define the root potential functions:

$$4\pi F_1 = Y_0(x_\pi) - R_\pi^{\frac{1}{2}} Y_0(x_{\Lambda_\pi}) - \tfrac{1}{2} R_\pi^{-\frac{1}{2}} (R_\pi - 1) Y(x_{\Lambda_\pi}) \tag{D1a}$$

$$4\pi F_2 = \tfrac{1}{2} Y(x_\pi) + \tfrac{1}{2} R_\pi^{-\frac{1}{2}} Y(x_{\Lambda_\pi}) + \frac{2}{R_\pi - 1} [R_\pi^{\frac{1}{2}} Y_0(x_{\Lambda_\pi}) - Y_0(x_\pi)]) \tag{D1b}$$

$$4\pi F_3 = \frac{1}{R_\pi - 1} [R_\pi^{\frac{1}{2}} Y_0(x_{\Lambda_\pi}) - Y_0(x_\pi)] + \tfrac{1}{2} R_\pi^{-\frac{1}{2}} Y(x_{\Lambda_\pi}) + \tfrac{1}{8} R_\pi^{-\frac{1}{2}} (R_\pi - 1) x_{\Lambda_\pi}^2 Y_1(x_{\Lambda_\pi}) \tag{D1c}$$

$$4\pi F_4 = b[\Lambda_\rho, m_\rho] \Big\{ \frac{1}{b[\Lambda_\rho, m_\pi]} Y_0(x_\pi) - \frac{R_\pi^{\frac{1}{2}}}{b[\Lambda_\rho, \Lambda_\pi]} Y_0(x_{\Lambda_\pi}) + \frac{b[\Lambda_\pi, m_\pi] R_\rho^{\frac{1}{2}}}{b[\Lambda_\rho, \Lambda_\pi] b[\Lambda_\rho, m_\pi]} Y_0(x_{\Lambda_\rho}) \Big\} \tag{D1d}$$

$$4\pi F_6 = \Big(\frac{m_\rho}{m_\pi}\Big)^3 \Big\{ Y_0(x_\rho) - R_\rho^{\frac{1}{2}} Y_0(x_{\Lambda_\rho}) - \tfrac{1}{2} R_\rho^{-\frac{1}{2}} (R_\rho - 1) Y(x_{\Lambda_\rho}) \Big\} \tag{D1e}$$

$$\begin{aligned} 4\pi F_7 = m_\rho m_\pi \Big\{ & \frac{b[\Lambda_\rho, m_\rho] R_\pi^{\frac{1}{2}}}{b[\Lambda_\rho, \Lambda_\pi] b[\Lambda_\pi, m_\rho]} Y_0(x_{\Lambda_\pi}) + \frac{b[\Lambda_\rho, m_\rho]}{b[\Lambda_\rho, m_\pi] b[m_\rho, m_\pi]} Y_0(x_\pi) \\ & - \frac{m_\rho b[\Lambda_\pi, m_\pi] R_\rho^{\frac{1}{2}}}{m_\pi b[\Lambda_\rho, \Lambda_\pi] b[\Lambda_\rho, m_\pi]} Y_0(x_{\Lambda_\rho}) - \frac{m_\rho b[\Lambda_\pi, m_\pi]}{m_\pi b[\Lambda_\pi, m_\rho] b[m_\rho, m_\pi]} Y_0(x_\rho) \Big\} \end{aligned} \tag{D1f}$$

$$4\pi F_8 = \Big(\frac{m_{a_1}}{m_\pi}\Big)^3 \Big\{ Y_0(x_{a_1}) - R_{a_1}^{\frac{1}{2}} Y_0(x_{\Lambda_{a_1}}) - \tfrac{1}{2} R_{a_1}^{-\frac{1}{2}} (R_{a_1} - 1) Y(x_{\Lambda_{a_1}}) \Big\} \tag{D1g}$$

where $R_M = (\Lambda_M/m_M)^2$ and $Y(x) = \exp(-x)$, $Y_0(x) = Y(x)/x$, $Y_1(x) = Y_0(x)(1 + 1/x)$, $Y_2(x) = Y_0(x)(1 + 3/x + 3/x^2)$, $Y_3(x) = Y_0(x)(1 + 6/x + 15/x^2 + 15/x^3)$, $b[\alpha, \beta] = \alpha^2 - \beta^2$, $x_\pi = m_\pi x$, $x_{\Lambda_\pi} = \Lambda_\pi x$, $x_\rho = m_\rho x$, $x_{\Lambda_\rho} = \Lambda_\rho x$, $x_{a_1} = m_{a_1} x$ and $x_{\Lambda_{a_1}} = \Lambda_{a_1} x$.

We now define the f_i in terms of the root potential functions with rules like,

$$f_8 = F_6[Y_0 \to Y_2, Y \to y Y_1; 1/m_\rho^2]. \tag{D2a}$$

The rule means that f_8 is equal to F_6 with Y_0 replaced by Y_2 and $Y(\xi)$ replaced by $\xi Y_1(\xi)$ where ξ can be any argument. Further, each term $\exp(-ax)$ becomes $(a/m_\rho)^2 \exp(-ax)$ which is indicated by the $1/m_\rho^2$ after the semi-colon.

$$f_1 = F_1[Y_0 \to Y_1, Y \to Y; 1/m_\pi] \tag{D2b}$$

$$f_2 = F_1[Y_0 \to Y_2, Y \to y Y_1; 1/m_\pi^2] \tag{D2c}$$

$$f_3 = f_1/x_\pi \tag{D2d}$$

$$f_4 = F_4[Y_0 \to Y_1; 1/m_\pi] \tag{D2e}$$

$$f_5 = F_4[Y_0 \to Y_2; 1/m_\pi^2] \tag{D2f}$$

$$f_6 = f_4/x_\pi \tag{D2g}$$

$$f_7 = F_6[Y_0 \to Y_0 + Y_1/y, Y \to Y - Y_0; 1/m_\rho^2] \tag{D2h}$$

$$f_8 = F_6[Y_0 \to Y_2, Y \to y Y_1; 1/m_\rho^2] \tag{D2i}$$

$$f_{11} = F_7[Y_0 \to Y_1; 1/m_\pi] \tag{D2j}$$

$$f_{12} = F_7[Y_0 \to Y_2; 1/m_\pi^2] \tag{D2k}$$

$$f_{13} = f_{11}/x_\pi \tag{D2l}$$
$$f_{14} = F_7[Y_0 \to Y_1 + Y_2/y; 1/m_\pi^3] \tag{D2m}$$
$$f_{15} = F_7[Y_0 \to Y_2; 1/m_\pi^4] \tag{D2n}$$
$$f_{16} = F_7[Y_0 \to Y_1/y; 1/m_\pi^4] \tag{D2o}$$
$$f_{17} = F_7[Y_0 \to Y_3; 1/m_\pi^3] \tag{D2p}$$
$$f_{18} = f_{12}/x_\pi \tag{D2q}$$

$$f_{19} = F_2[Y_0 \to Y_3, Y \to yY_2; 1/m_\pi^3] \tag{D2r}$$
$$f_{20} = F_2[Y_0 \to Y_2/y, Y \to Y_1; 1/m_\pi^3] \tag{D2s}$$

$$f_{21} = F_3[Y_0 \to Y_3, Y \to yY_2, y^2Y_1 \to y^2Y_1; 1/m_\pi^3] \tag{D2t}$$
$$f_{22} = F_3[Y_0 \to Y_2/y, Y \to Y_1, y^2Y_1 \to Y; 1/m_\pi^3] \tag{D2u}$$

$$f_{23} = F_8[Y_0 \to Y_2, Y \to yY_1; 1/m_{a_1}^2] \tag{D2v}$$
$$f_{24} = F_8[Y_0 \to Y_1/y, Y \to Y_0; 1/m_{a_1}^2] \tag{D2w}$$

$$f_{25} = F_2[Y_0 \to Y_1, Y \to Y; 1/m_\pi] \tag{D2x}$$
$$f_{26} = F_2[Y_0 \to Y_2, Y \to yY_1; 1/m_\pi^2]. \tag{D2y}$$

The functions e_i are given by,

$$8\pi e_2 = \frac{1}{x_\pi}[e_{11}(m_\pi) - e_{11}(\Lambda_\pi) + (R_\pi - 1)e_{12}(\Lambda_\pi)] \tag{D3}$$

$$8\pi e_3 = e_{31}(m_\pi) - e_{31}(\Lambda_\pi) + (R_\pi - 1)e_{32}(\Lambda_\pi) \tag{D4}$$

where,

$$e_{11}(m) = \int_0^1 dt\ \exp(-cx)[j_0 + \tfrac{Qt}{c} j_1] \tag{D5}$$

$$e_{12}(m) = -\frac{m_\pi^2}{2}\int_0^1 dt\ \exp(-cx)[\tfrac{x}{c} j_0 + \tfrac{Qt}{c^3}(1+cx)j_1] \tag{D6}$$

$$e_{31}(m) = \frac{1}{m_\pi}\int_0^1 dt\ \exp(-cx)[(\tfrac{1}{x} + c - \tfrac{Q^2t^2}{c})j_0 + Qt(\tfrac{3}{cx} + 2)j_1] \tag{D7}$$

$$e_{32}(m) = -\frac{m_\pi}{2}\int_0^1 dt\, \frac{\exp(-cx)}{c}[(cx - \tfrac{Q^2t^2}{c^2}(1+cx))j_0 + \tfrac{Qt}{c}(2cx + 3 + \tfrac{3}{cx})j_1], \tag{D8}$$

the argument of the bessel functions is Qtx and the m dependence comes from c which is given by

$$c(m) = [Q^2 t(1-t) + m^2]^{\frac{1}{2}}. \tag{D9}$$

The functions d_i are given by,

$$d_2 = \tfrac{1}{2} F_1 d_3 = \tfrac{1}{2} x_\pi f_1 d_5 = \tfrac{1}{2} x_\pi f_2. \tag{D10}$$

APPENDIX E: CONSTRUCTION OF OBEP

The exchange of π, ρ and a_1 mesons leads to an isospin dependent NN potential with tensor and spin-spin components. The non-relativistic momentum space potentials between two nucleons labeled 1 and 2 were taken to be,

$$V^\pi = -3c_\pi \, \tau_1 \cdot \tau_2 \, \frac{(\sigma_1 \cdot Q_2)(\sigma_2 \cdot Q_2)}{m_\pi^2} \frac{\Delta_F^\pi(Q_2)}{m_\pi} F_{\pi NN}^2(Q_2) \tag{E1a}$$

$$V^\rho = -3c_\rho \, \tau_1 \cdot \tau_2 \, \frac{(\sigma_1 \times Q_2) \cdot (\sigma_2 \times Q_2)}{m_\rho^2} \times \frac{\Delta_F^\rho(Q_2)}{m_\rho} F_{\rho NN}^2(Q_2) \left(\frac{m_\rho}{m_\pi}\right)^3 \tag{E1b}$$

$$V^{a_1} = -3c_{a_1} \, \tau_1 \cdot \tau_2 \, \left[\sigma_1 \cdot \sigma_2 + \frac{(\sigma_1 \cdot Q_2)(\sigma_2 \cdot Q_2)}{m_{a_1}^2}\right] \times \frac{\Delta_F^{a_1}(Q_2)}{m_{a_1}} F_{a_1 NN}^2(Q_2) \left(\frac{m_{a_1}}{m_\pi}\right)^3 \tag{E1c}$$

where,

$$c_\pi = c_{a_1} = m_\pi f_{\pi NN}^2 / 3 \tag{E2a}$$

$$c_\rho = \frac{m_\pi}{3} g_{\rho NN}^2 (1 + \kappa_V)^2 \left(\frac{m_\pi}{2M}\right)^2 . \tag{E2b}$$

The configuration representation of these potentials are, (with $M = \pi, \rho, a_1$),

$$V^M(x) = c_M [V_T^M(x) S_{12} + V_S^M(x) \sigma_1 \cdot \sigma_2] \tag{E3}$$

where,

$$S_{12} = 3(\sigma_1 \cdot \hat{x})(\sigma_2 \cdot \hat{x}) - \sigma_1 \cdot \sigma_2 \tag{E4}$$

and,

$$V_T^\pi(x) = F_\pi^{''} - F_\pi^{'} / x_\pi \tag{E5a}$$

$$V_T^\rho(x) = -(F_\rho^{''} - F_\rho^{'} / x_\rho) \tag{E5b}$$

$$V_T^{a_1}(x) = F_{a_1}^{''} - F_{a_1}^{'} / x_{a_1} \tag{E5c}$$

$$V_S^{\pi}(x) = F_{\pi}^{''} + 2F_{\pi}^{'}/x_{\pi} \tag{E5d}$$

$$V_S^{\rho}(x) = -2(F_{\rho}^{''} + 2F_{\rho}^{'}/x_{\rho}) \tag{E5e}$$

$$V_S^{a_1}(x) = F_{a_1}^{''} + 2F_{a_1}^{'}/x_{a_1} - 3F_{a_1} \tag{E5f}$$

with,

$$F_M = \frac{1}{2\pi^2 x_M} \int_0^{\infty} \frac{q\sin(qx)}{q^2+m_M^2} F_{MNN}^2(q) \left(\frac{m_M}{m_\pi}\right)^3 . \tag{E6}$$

The notation $F_M^{'}$ means $d/dx_M F_M$. With monopole form factors, $F_M NN(q) = (\Lambda_M^2 - m_M^2)/(\Lambda_M^2 + q^2)$ we found that,

$$\begin{aligned} 4\pi\, V_T^M(x) = (-1)^{\delta(M,\rho)} \left(\frac{m_M}{m_\pi}\right)^3 \times [&Y_2(m_M x) - R_M^{\frac{3}{2}} Y_2(\Lambda_M x) \\ &-R_M^{\frac{1}{2}}(R_M - 1)\, \Lambda_M x\, Y_1(\Lambda_M x)] \end{aligned} \tag{E7}$$

$$4\pi\, V_S^{\pi}(x) = Y_0(m_\pi x) - R_\pi^{\frac{1}{2}} Y_0(\Lambda_\pi x) - R_\pi^{-\frac{1}{2}} (R_\pi - 1)\, Y(\Lambda_\pi x) \tag{E8}$$

$$4\pi\, V_S^{\rho}(x) = (-2) \left(\frac{m_\rho}{m_\pi}\right)^3 [Y_0(m_\rho x) - R_\rho^{\frac{1}{2}} Y_0(\Lambda_\rho x) - R_\rho^{\frac{1}{2}} (R_\rho - 1)\, Y(\Lambda_\rho x)] \tag{E9}$$

$$\begin{aligned} 4\pi\, V_S^{a_1}(x) = (-2) \left(\frac{m_{a_1}}{m_\pi}\right)^3 [&Y_0(m_{a_1} x) - R_{a_1}^{\frac{1}{2}} Y_0(\Lambda_{a_1} x) \\ &-\frac{R_{a_1}^{-\frac{1}{2}}}{4}(R_{a_1} - 1)(R_{a_1} - 3)\, Y(\Lambda_{a_1} x)]. \end{aligned} \tag{E10}$$

Our exchange potentials for π and ρ are the same as those used by others [32,16]. Our exchange potential for a_1 agrees with that of Ref. [32] but not with that of Ref. [33]. The difference is that the $(\sigma_1 \cdot Q_2)(\sigma_2 \cdot Q_2)$ term was left out in [33]. Here we include this term because we found that it contributes non-negligibly: $V_T^a(x)$ is entirely due to the term and $V_S^a(x)$ would be $\approx 50\%$ smaller at $x = 1/\Lambda_{a_1}$ and 50% larger for $x \gg 1/\Lambda_{a_1}$ without the term.

FIGURES

FIG. 1. Examples of nuclear densities. Points were also calculated at x=5.5,6.5 and 7.5 fm but are not shown.

FIG. 2. Isospin dependent spin-spin and tensor potentials from pion exchange and first and second derivatives $F_\pi^{'}$ and $F_\pi^{''}$. The solid line is for $\Lambda_\pi = 1.2$ GeV and the dashed line for $\Lambda_\pi = \infty$. The constant c_π has been set to one for these graphs.

FIG. 3. Variation of observables with the nucleon pseudoscalar coupling g_P.

FIG. 4. Potential function for the π pair term of the vector current. The pion cutoff is $\Lambda_\pi = 1200$ Mev

TABLES

TABLE I. Effective couplings in the EPM and IA and their difference. The uncertainty in G_{P} reflects experimental uncertainty only.

Model	G_{V}		G_{P}		G_{A}	
EPM	0.85 ± 0.01		0.603 ± 0.001		1.29 ± 0.01	
IA	0.84	–1%	0.523	–13%	1.19	–8%

TABLE II. Origin of contributions to effective couplings

	G_{V}	G_{P}	G_{A}
Dominant	ρ_{V}	$\vec{j}_{\mathrm{A}}, \vec{j}_{\mathrm{V}}$	$\vec{j}_{\mathrm{A}}$
Other	$\vec{j}_{\mathrm{V}}$	ρ_{A}	$\rho_{\mathrm{A}}, \vec{j}_{\mathrm{V}}$

TABLE III. Labeling of reduced matrix elements. The superscript in the isospin part means $()^{-} = \frac{1}{2}[()^{x} - i()^{y}]$.

Z	S_{Σ}	$\mathcal{I}$
A	$\mathbb{1}$	$12i(\tau_2 \times \tau_3)^{-}$
B	$\vec{\sigma}_3$	$12i(\tau_2 \times \tau_3)^{-}$
C	$[\sigma_2 \otimes \sigma_3]_0$	$12i(\tau_2 \times \tau_3)^{-}$
D	$[\sigma_2 \otimes \sigma_3]_1$	$12i(\tau_2 \times \tau_3)^{-}$
E	$[\sigma_2 \otimes \sigma_3]_2$	$12i(\tau_2 \times \tau_3)^{-}$
F	$\vec{\sigma}_3$	$12\tau_3^{-}$
G	$[\sigma_2 \otimes \sigma_3]_0$	$12\tau_3^{-}$
H	$[\sigma_2 \otimes \sigma_3]_1$	$12\tau_3^{-}$
I	$[\sigma_2 \otimes \sigma_3]_2$	$12\tau_3^{-}$

TABLE IV. Sizes of matrix elements. The Bessel function in y has been expanded and only the first term kept except in the cases of $D^1_{000}, D^1_{202}, F^1_{000}$ and F^1_{202}. The dominant overlap describes the total orbital angular momentum of the wavefunction components which contribute most to the matrix element.

Matrix element		Integral		Dominant overlap(s)
	AV14+3BF[8]	AV14[8]	AV14+3BF[22]	
D^1_{000}	9.62	9.57	9.63	SS
G^0_{000}	5.78	5.96	5.77	SS
F^1_{000}	–3.55	–3.53	–3.55	SS
D^1_{202}	2.03	1.99	2.05	SD
F^1_{202}	–0.900	–0.867	–0.907	SD
I^0_{202}	–0.066	–0.056	–0.082	SD,DD
E^1_{110}	0.20	0.20	0.20	SD
I^0_{110}	–0.15	–0.15	–0.15	SD
F^1_{110}	0.14	0.14	0.14	SD
B^0_{111}	0.057	0.061	0.054	DD
G^0_{110}	0.045	0.053	0.044	SS,DD
A^1_{111}	0.035	0.037	0.025	DD
C^1_{111}	–0.024	–0.023	–0.031	DD
F^1_{110}	–0.017	–0.018	–0.017	SS,DD
E^1_{111}	–0.012	–0.014	–0.012	DD,SP
H^0_{111}	0.004	0.003	0.000	SP
D^1_{022}	–0.017	–0.017	–0.017	SD
F^1_{022}	0.005	0.005	0.005	SD
I^0_{022}	–0.001	–0.001	–0.001	DD
${}_xD^1_{000}$	–7.00	–6.79	–7.02	SS
${}_xB^1_{000}$	–0.44	–0.45	–0.44	SS
${}_xH^1_{000}$	0.31	0.32	0.31	SS
${}_xD^1_{202}$	–1.82	–1.77	–1.84	SD
${}_xB^1_{202}$	–0.49	–0.48	–0.49	SD
${}_xH^1_{202}$	0.38	0.38	0.38	SD
${}_xI^1_{202}$	0.023	0.019	0.023	SD
${}_xD^{011}_{101}$	1.3	1.2	1.3	SD
${}_xB^{011}_{101}$	0.94	0.90	0.94	SD
${}_xH^{011}_{101}$	–0.66	–0.62	–0.66	SD
${}_xD^{111}_{101}$	–1.1	–1.1	–1.1	SD
${}_xB^{111}_{101}$	–0.79	–0.77	–0.79	SD
${}_xH^{111}_{101}$	0.55	0.54	0.55	SD
${}_xD^{211}_{101}$	0.29	0.28	0.29	SD
${}_xB^{211}_{101}$	0.19	0.20	0.19	SD
${}_xH^{211}_{101}$	–0.14	–0.14	–0.13	SD
${}_xG^{111}_{101}$	0.033	0.036	0.032	DD
${}_xI^{111}_{101}$	–0.021	–0.022	–0.21	SD,DD
${}_xI^{211}_{101}$	–0.023	–0.024	–0.025	DD

TABLE V. Trion isovector magnetic moment: (a) AV14, 8 channel $\langle\,^3\mathrm{H} \mid {}^3\mathrm{H}\rangle$ (b) AV14, 8 channel $\langle\,^3\mathrm{H} \mid {}^3\mathrm{He}\rangle$ (c) AV14+3BF, 8 channel $\langle\,^3\mathrm{H} \mid {}^3\mathrm{He}\rangle$ (d) AV14+3BF, 22 channel $\langle\,^3\mathrm{H} \mid {}^3\mathrm{He}\rangle$

	Ref. [5]	(a)	(b)	(c)	(d)
IA	–2.172	–2.177	–2.174	–2.175	–2.175
pair	–0.290	–0.288	–0.285	–0.298	–0.298
pion	0.092	0.096	0.095	0.100	0.101
delta	–0.099	–0.100	–0.098	–0.104	–0.105
total	–2.469	–2.468	–2.462	–2.477	–2.477

TABLE VI. Trion Gamow-Teller matrix element. The entries labeled AHHST are taken from Ref. [3] and use wavefunctions found from the Paris potential.

Current	AHHST	local	AHHST	non-local	AHHST
AP1+AP7	[2a,vert]	0.000	0.000	–0.016	–0.015
AP3	[2a,ret]	0.000	0.000	–0.008	–0.007
AP4	[2a,form]	0.000	0.000	–0.002	–0.001
APSPV	[2a,PS–PV]	0.000	0.000	0.016	0.015
AP5	[2d]	0.022	0.019	0.004	0.003
ANP1	[2c]	–0.013	–0.011	0.000	–0.001
ANP2	[2b]	0.009	0.007	0.003	0.003
one-body	one-body	0.924	0.927	0.000	0.000

TABLE VII. Ranges of parameters for the meson exchange currents.

Parameter	range
κ_V	3.7 - 6.6
$g^2_{\rho NN}/4\pi$	0.70 - 0.95
G_1	2.2 - 2.6
λ	0 - 1
$f^2_{\pi NN}/4\pi$	0.075 - 0.081
Λ_π	1.0 - 1.5 GeV
$f^2_{\pi N\Delta}/4\pi$	0.23 - 0.36

TABLE VIII. Strong form factor fit for two values of rho anomalous coupling κ_V. The values of $f^2_{\pi NN}/4\pi$ and $g^2_{\rho NN}/4\pi$ are 0.081 and 0.95 respectively. The formfactors are given in GeV.

	$\kappa_V = 3.7$		$\kappa_V = 6.6$	
Λ_π	Λ_ρ	Λ_a	Λ_ρ	Λ_a
1.0	1.86	1.09 - 1.86	1.18	1.09 - 1.18
1.2	2.23	1.09 - 2.23	1.25	1.09 - 1.25
1.5	2.76	1.09 - 2.76	1.33	1.09 - 1.33

TABLE IX. Results for the rate and spin observables.

	AV14+3BF [22]	AV14+3BF [8]	AV14 [8]	EPM Ref. [1]
Γ_0 [s^{-1}]	1502 ± 32	1498	1456	1497 ± 21
A_v	0.515 ± 0.005	0.515	0.516	0.524 ± 0.006
A_t	–0.375 ± 0.004	–0.375	–0.373	–0.379 ± 0.004
A_Δ	–0.110 ± 0.006	–0.110	–0.110	–0.097 ± 0.007

TABLE X. Results for the rate and spin observables. The one-body currents are taken from the 22 channel AV14+3BF wavefunctions.

	AV14+3BF [22]	AV14+3BF [8]	AV14 [8]
Γ_0 [s^{-1}]	1502	1501	1491
A_v	0.515	0.516	0.518
A_t	–0.375	–0.375	–0.374
A_Δ	–0.110	–0.110	–0.108

TABLE XI. Contributions of each current ($\times 10^3$) to the current amplitudes and effective form factors.

Current	j_σ	$j_x^{(2)}$	ρ_1	j_Q	$j_x^{(1)}$	ρ_0	G_V	G_A	G_P
IA	877	–326	10	15	200	820	835	1185	516
AP1+AP7	–17							–17	
AP2+AP6	–6	–19							19
AP3	–8							–8	
AP4	–3							–3	
APSPV	8							8	
AP5	22		1.1					22	–1
ANP1	–13		–0.1					–13	
ANP2	8		0.4					8	
ANP3	–2	–5							5
ANP4	77	4						75	–4
ANP5	–29							–29	
ANP6	2							2	
VP1					64			64	64
VP2					–8			–8	–8
VNP1					16			16	16
VNP2					–6			–6	–6
total	918	–346	12	15	267	820	835	1300	601
EPM	928	–372	11	15	241	839	854	1293	603

TABLE XII. The split into local and non-local contributions. Only those currents which receive contributions from both local and non-local currents are included.

Current	$j_\sigma (\times 10^3)$		$j_x^{(2)} (\times 10^3)$	
	local	non-local	local	non-local
AP2+AP6	–4.2	–2.1	–12.6	–6.4
AP5	18.9	3.1		
ANP1	–12.8	0.2		
ANP2	6.2	2.2		
ANP3	–1.2	–0.4	–3.6	–1.1

TABLE XIII. Sensitivity of observables $\mathcal{O}$ to g_P.

$\mathcal{O}$	$\left\| \frac{g_P}{\mathcal{O}} \frac{d\mathcal{O}}{dg_P} \right\|_{g_P^{\mathrm{PCAC}}}$
Γ_0	0.11
A_v	0.37
A_t	0.73
A_Δ	0.75

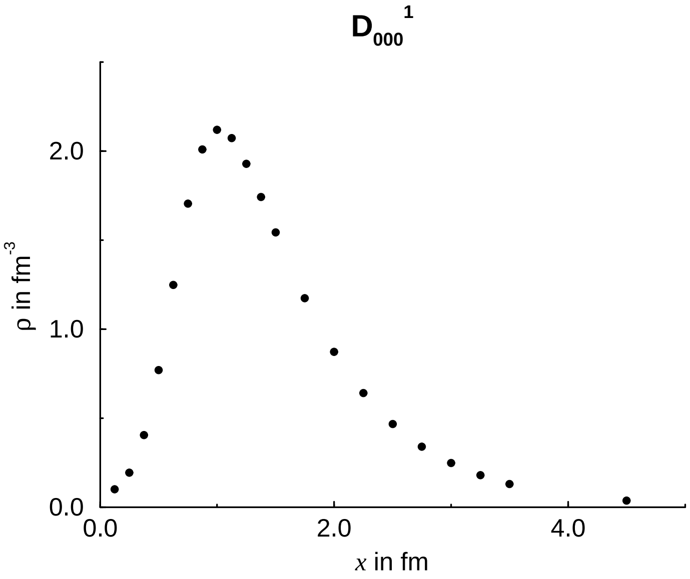
D_{000}^{1}
ρ in fm^{-3}
0.0
1.0
2.0
0.0
2.0
4.0
x in fm

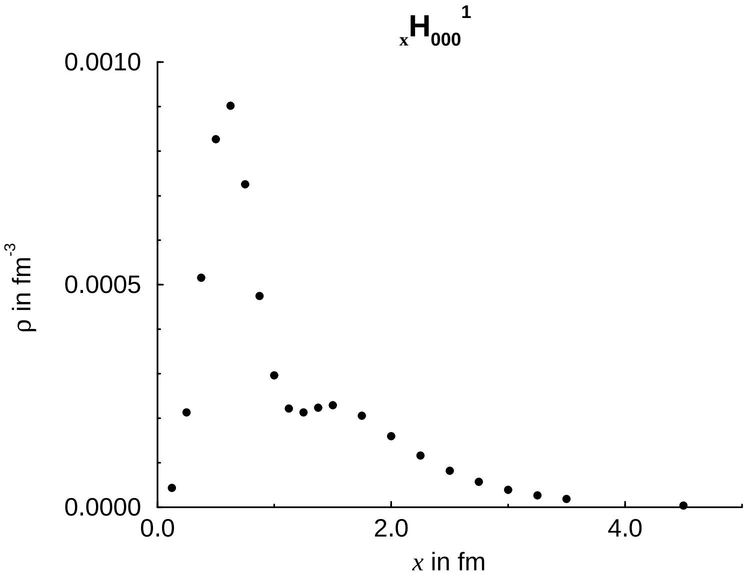
$_{x}H_{000}^{1}$
ρ in fm^{-3}
0.0000
0.0005
0.0010
0.0
2.0
4.0
x in fm

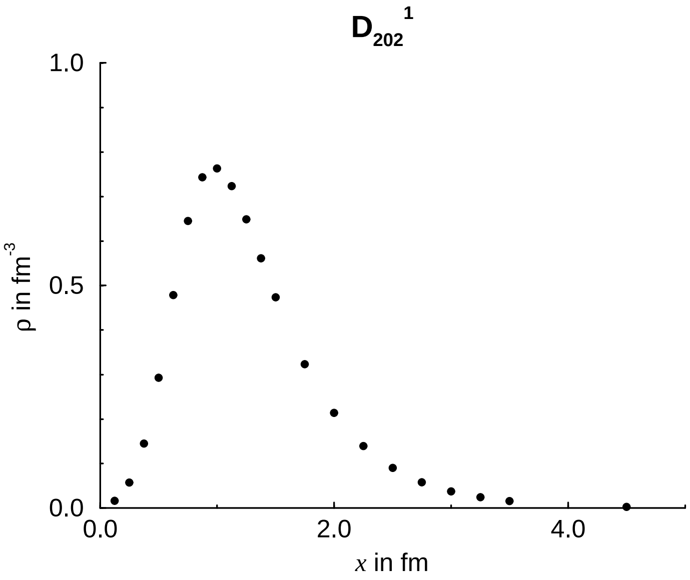
D_{202}^{1}
ρ in fm^{-3}
0.0
0.5
1.0
0.0
2.0
4.0
x in fm

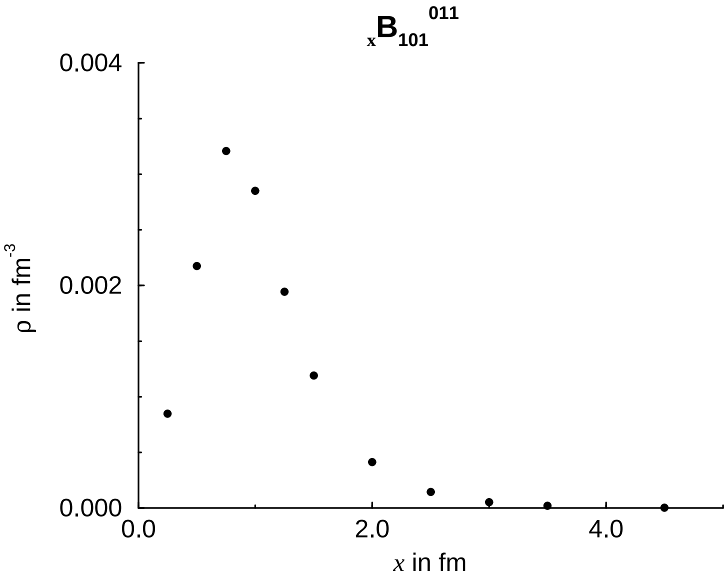
$_{x}B_{101}^{011}$
ρ in fm^{-3}
0.000
0.002
0.004
0.0
2.0
4.0
x in fm

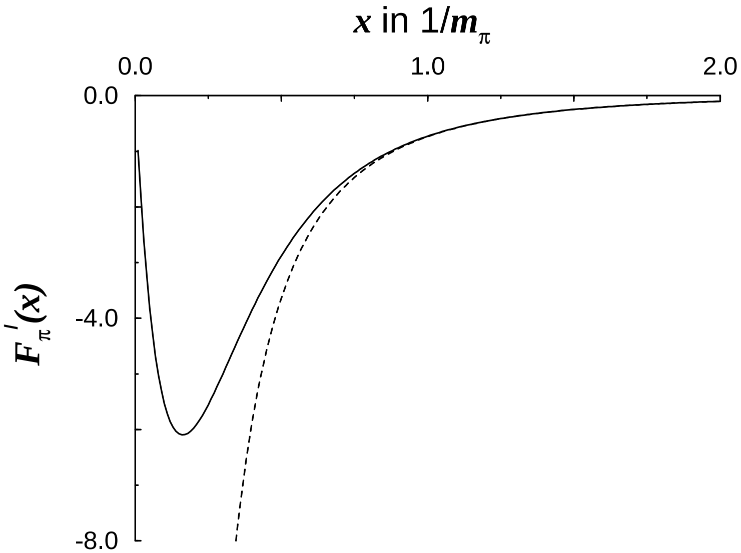
x in $1/m_\pi$
0.0
1.0
2.0
0.0
-4.0
-8.0
$F_\pi^{I}(x)$

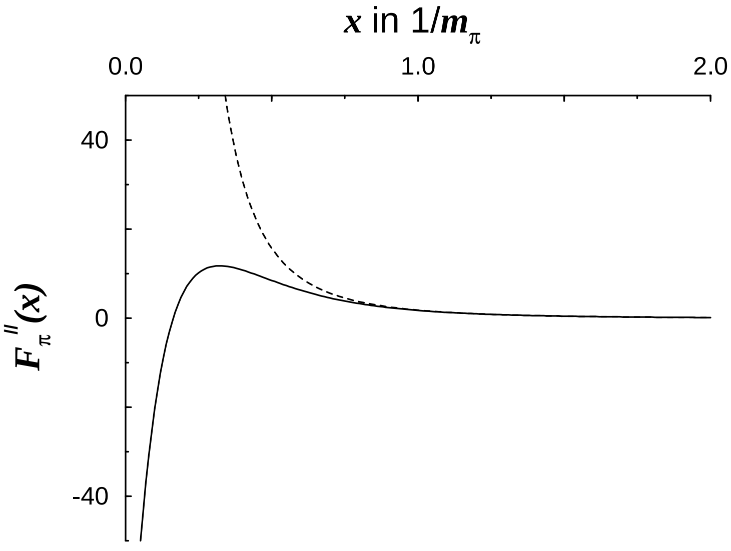
x in $1/m_\pi$
0.0
1.0
2.0
40
0
-40
$F_\pi^{II}(x)$

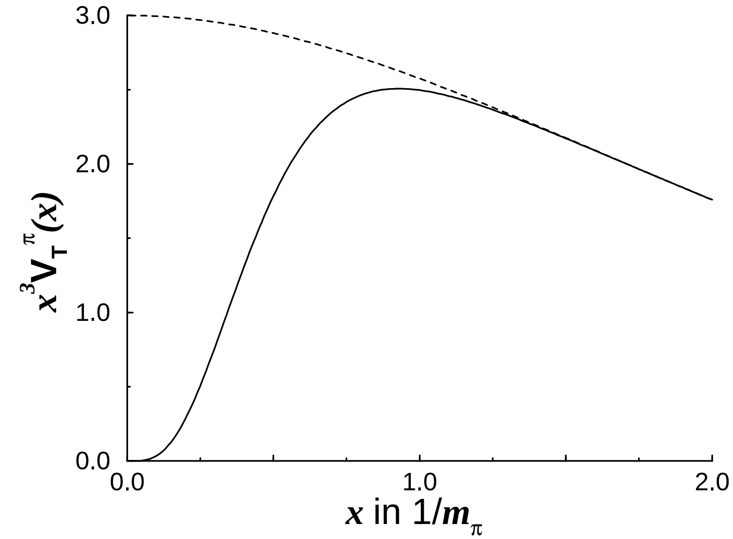
3.0
2.0
1.0
0.0
$x^3 V_T^\pi(x)$
0.0
1.0
2.0
x in $1/m_\pi$

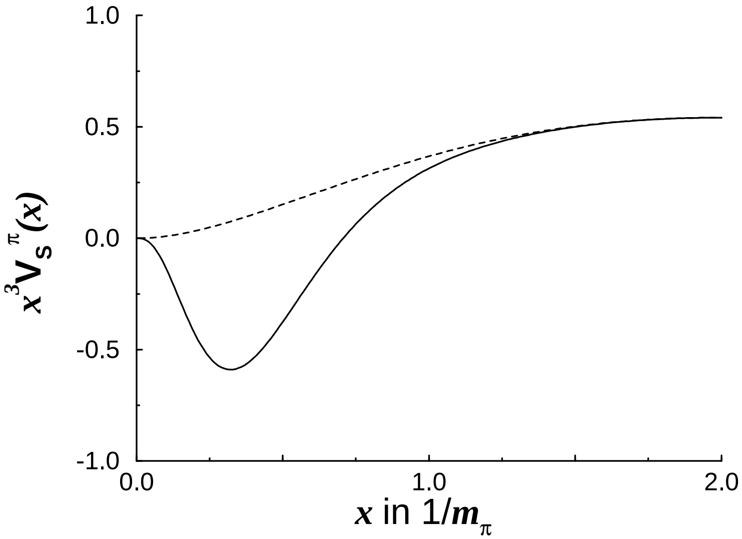
1.0
0.5
0.0
-0.5
-1.0
$x^3 V_S^\pi(x)$
0.0
1.0
2.0
x in $1/m_\pi$

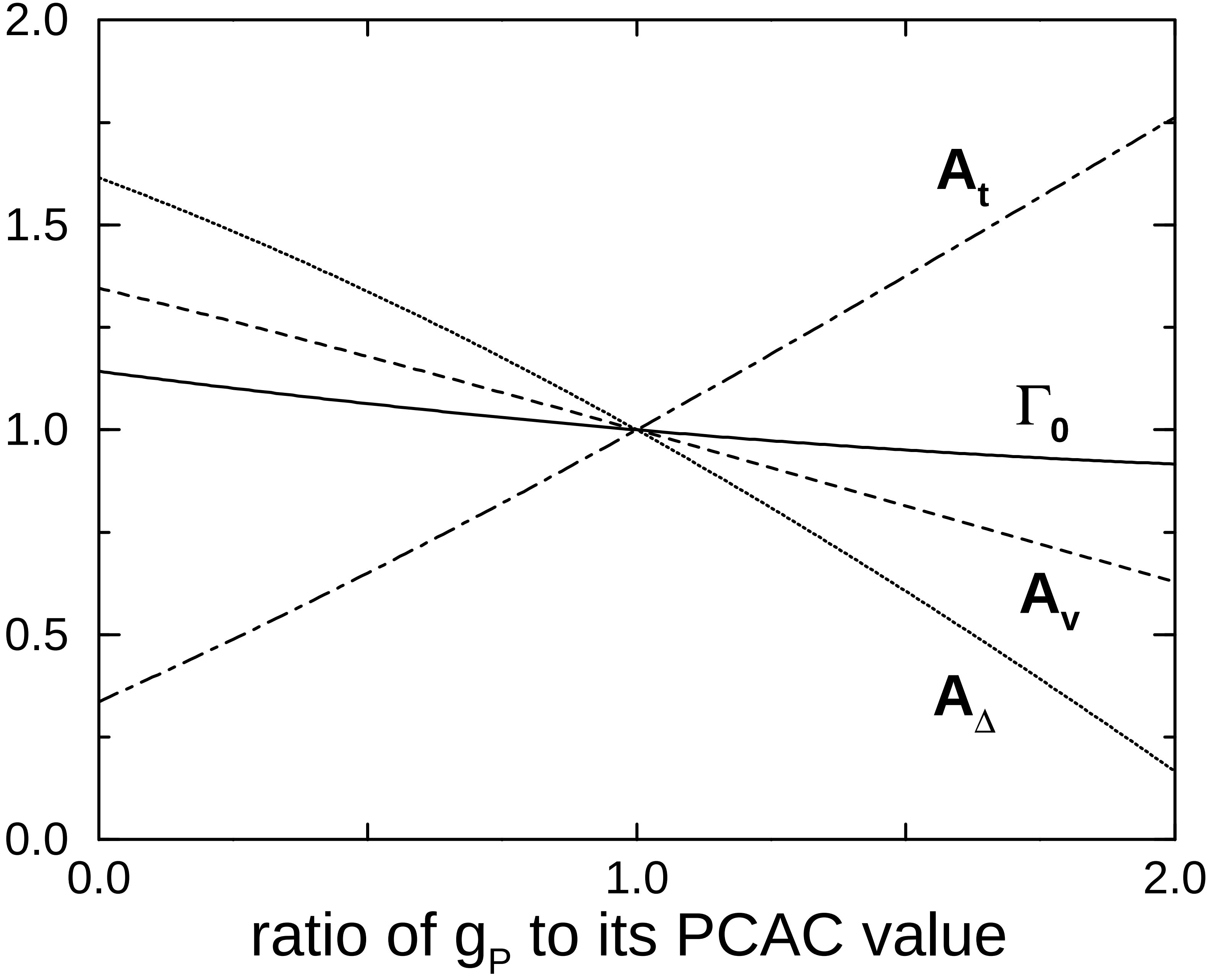
2.0
1.5
1.0
0.5
0.0
0.0
1.0
2.0
ratio of g_P to its PCAC value
A_t
Γ_0
A_v
A_Δ

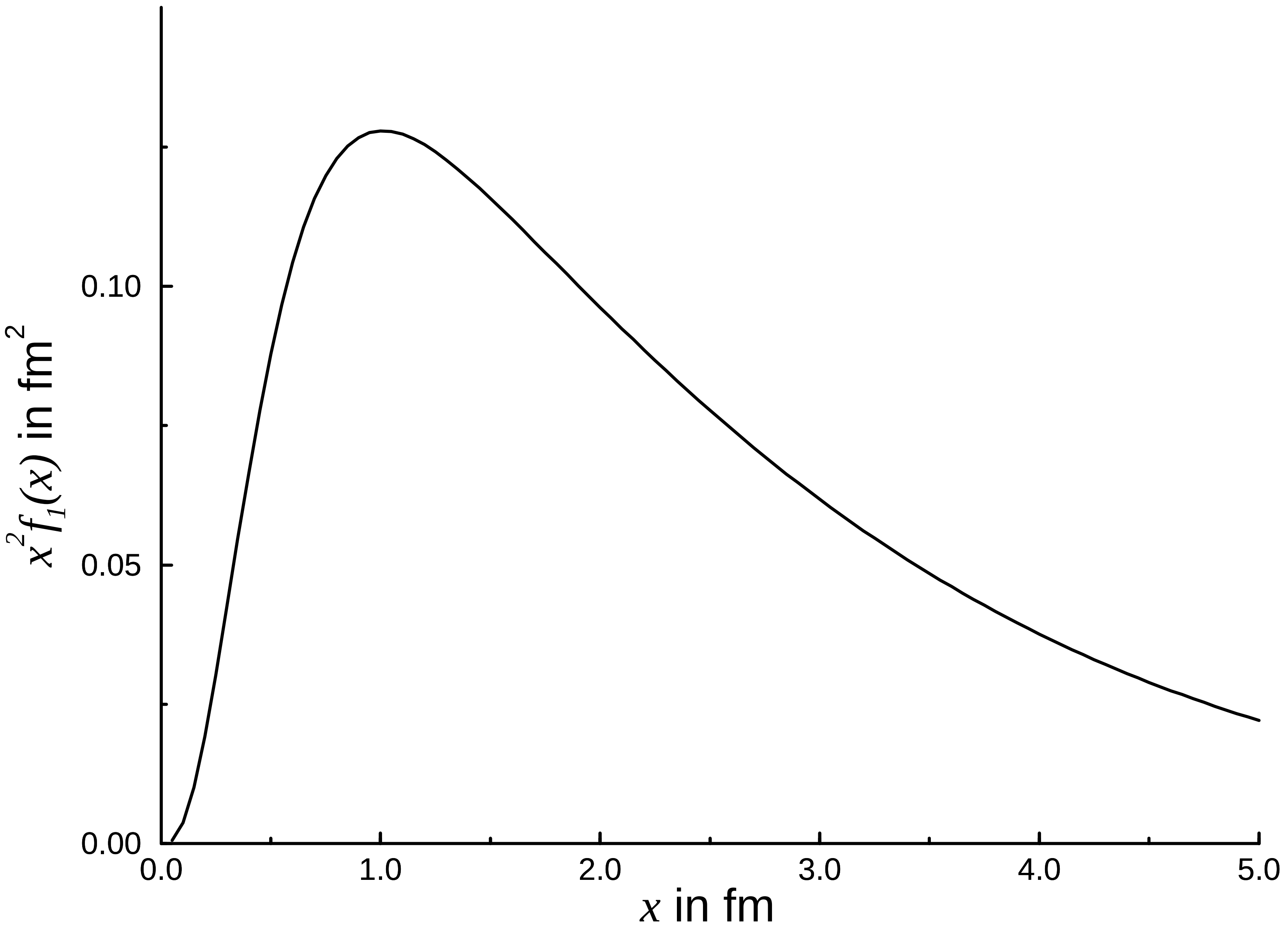
0.00
0.05
0.10
0.0
1.0
2.0
3.0
4.0
5.0
$x^2 f_1(x)$ in fm^2
x in fm